Kappa Opioid Receptor Antagonism Restores Phosphorylation, Trafficking and Behavior induced by a Disease Associated Dopamine Transporter Variant

Running Title: κ-Opioid Receptor Antagonism Normalizes DAT Val559

Felix P. Mayer, PhD[1,2,%], Adele Stewart, PhD[1,2], Durairaj Ragu Varman, PhD[3], Amy E. Moritz, PhD[4], James D. Foster, PhD[4], Anthony W. Owens[5], Lorena B. Areal, PhD[1], Raajaram Gowrishankar, PhD[1#], Michelle Velez[1], Kyria Wickham[1], Hannah Phelps[1], Rania Katamish[1], Maximilian Rabil[1], Lankupalle D. Jayanthi, PhD[3], Roxanne A. Vaughan, PhD[4], Lynette C. Daws, PhD[5,6], Randy D. Blakely, PhD[1,2]*, and Sammanda Ramamoorthy, PhD[3]*

[1] Department of Biomedical Science, Charles E. Schmidt College of Medicine, Florida Atlantic University, Jupiter, FL, USA.

[2] Stiles-Nicholson Brain Institute, Florida Atlantic University, Jupiter, FL, USA.

[3] Department of Pharmacology and Toxicology, Virginia Commonwealth University, Richmond, VA, USA

[4] Department of Biomedical Sciences, University of North Dakota School of Medicine and Health Sciences, Grand Forks, ND, USA

[5] Department of Cellular and Integrative Physiology, University of Texas Health Science Center at San Antonio, TX, USA

[6] Department of Pharmacology, University of Texas Health Science Center, San Antonio, TX, USA.

#present address: Departments of Anesthesiology and Pain Medicine and Pharmacology, University of Washington, Seattle, WA, USA and Center for the Neurobiology of Addiction, Pain and Emotion, University of Washington, Seattle, WA, USA

%present address: Department of Neuroscience, Faculty of Health and Medical Sciences, University of Copenhagen, Copenhagen, DK-2200, Denmark.

*to whom correspondence should be addressed:

sammanda.ramamoorthy@vcuhealth.org
Professor, Department of Pharmacology & Toxicology Virginia Commonwealth University R. Blackwell Smith Building, Room 756A P.O. Box 980613 410 North, 12th Street (at Clay St.) Richmond, VA 23298-0613, USA; Tel: 804-828-8407; Fax: 804-828-2117

rblakely@health.fau.edu
Professor, FAU Stiles-Nicholson Brain Institute David J.S. Nicholson Distinguished Professor in Neuroscience, Dept Biomedical Science Charles E. Schmidt College of Medicine 5353 Parkside Drive, Jupiter, FL 33458, USA MC-22/ Room 201G, Tel: 561-799-8100

Abstract

Aberrant dopamine (DA) signaling is implicated in schizophrenia, bipolar disorder (BPD), autism spectrum disorder (ASD), substance use disorder, and attention-deficit/hyperactivity disorder (ADHD). Treatment of these disorders remains inadequate, as exemplified by the therapeutic use of d-amphetamine and methylphenidate for the treatment of ADHD, agents with high abuse liability. In search for an improved and non-addictive therapeutic approach for the treatment of DA-linked disorders, we utilized a preclinical mouse model expressing the human DA transporter (DAT) coding variant DAT Val559, previously identified in individuals with ADHD, ASD, or BPD. DAT Val559, like several other disease-associated variants of DAT, exhibits anomalous DA efflux (ADE) that can be blocked by d-amphetamine and methylphenidate. Kappa opioid receptors (KORs) are expressed by DA neurons and modulate DA release and clearance, suggesting that targeting KORs might also provide an alternative approach to normalizing DA-signaling disrupted by perturbed DAT function. Here we demonstrate that KOR stimulation leads to enhanced surface trafficking and phosphorylation of Thr53 in wildtype DAT, effects achieved constitutively by the Val559 mutant. Moreover, these effects can be rescued by KOR antagonism of DAT Val559 in *ex vivo* preparations. Importantly, KOR antagonism also corrected *in vivo* DA release as well as sex-dependent behavioral abnormalities observed in DAT Val559 mice. Given their low abuse liability, our studies with a construct valid model of human DA associated disorders reinforce considerations of KOR antagonism as a pharmacological strategy to treat DA associated brain disorders.

Introduction

Dopamine (DA) is a powerful neuromodulator whose actions impact multiple fundamental behaviors, including novelty and reward salience (1), motivation and attention (2), motor initiation and coordination (3) and executive function (4), among others. Accordingly, altered DA signaling has been implicated in multiple neuropsychiatric disorders such as attention-deficit/hyperactivity disorder (ADHD) (5), autism spectrum disorder (ASD) (6), bipolar disorder (BPD) (7), Parkinson's disease (8), schizophrenia (9) and substance use disorders (10), though the detailed molecular underpinnings of these conditions remain areas of intense investigation. The presynaptic DA transporter (DAT, *SLC6A3*) tightly regulates the spatiotemporal availability of extracellular DA (11) and aids in replenishing vesicular storages of DA by acting in concert with the *de novo* synthesis machinery (12,13). Abnormal DAT availability in humans with neuropsychiatric disorders has been reported (14,15) and first line treatments for ADHD, i.e., methylphenidate and alpha-methylphenethylamine (d-amphetamine) formulations (16) exhibit high affinity towards DAT (11) and modulate extracellular DA in human subjects (17). Moreover, given abnormal behavior of DAT-manipulated animals (12,18–24) and that the DAT gene *SLC6A3* is implicated in neuropsychiatric diseases (25), ample evidence identifies DAT as a direct contributor to pathological DA dysregulation.

A role of altered DAT function in neuropsychiatric disorders has been advanced by the identification of rare missense variants in the *SLC6A3* gene that encodes DAT in individuals diagnosed with ADHD (26–28), BPD (29) and ASD (30–32). Importantly, these variants have been shown to modulate DAT function (27,28,30,33,34) and/or expression of DAT on the cell surface (27,33,35), and thus are expected to perturb extracellular DA clearance *in vivo*. We and colleagues identified the DAT Ala559Val substitution in two male siblings with ADHD (26), and two unrelated males with ASD (32), a disorder with significant ADHD comorbidity (36–38). Grunhage and coworkers also observed expression of the variant in a girl with BPD (29), a disorder also demonstrating significant familial co-morbidity and shared genetics (39,40). When expressed in a heterologous cell model, DAT Val559 displays normal transporter protein expression, surface abundance and DA uptake rates (33,41). Conspicuously, however, the variant exhibits anomalous DA efflux (ADE) when transfected cells are preloaded with DA (41,42) and increased lateral mobility on the cell surface (43), suggestive of alterations in DAT-associated proteins that influence transporter localization and transport dynamics. DAT dependence of DAT Val559-mediated ADE was established through a block of efflux by methylphenidate and amphetamine, as well as cocaine (41,42). Interestingly, ADE has now been recognized as a functional correlate of multiple disease-associated DAT variants

87 (21,30,34,41,42) and can also be triggered in wildtype (WT) DAT via G protein interactions (44,45),
88 extending the ADE phenotype beyond that seen with rare genetic variants.
89
90 *In vivo*, DAT Val559 KI mice (18,46) were found to display normal total DAT expression, as well as DA
91 uptake and tissue DA levels that were indistinguishable from those observed in WT mice (18). In
92 accordance with ADE, however, the striatum of these mice was found to exhibit tonically elevated
93 extracellular DA levels *in vivo* that supports constitutive D2-type autoreceptor (D2AR) activation and
94 blunted vesicular DA release. In keeping with these changes, DAT Val559 mice have been shown to display
95 blunted locomotor responses to methylphenidate and d-amphetamine, heightened locomotor responses
96 to imminent handling, i.e. darting (18), enhanced motivation for reward and waiting impulsivity (19),
97 altered working memory (24) and compulsive reward seeking (23). Together these findings document the
98 value of DAT Val559 mice as a construct-valid model of endogenous alterations in synaptic DA
99 homeostasis that arise from DAT dysfunction. Moreover, the DAT Val559 model provides an *in vivo*
100 platform for the preclinical evaluation of novel therapeutic strategies to ameliorate synaptic DA-
101 associated neurobehavioral disorders, with a particular need for agents without addictive potential.
102
103 Various mechanisms have been identified that modulate DAT activity via protein-protein interactions
104 (44,47–49) and post-translational modifications (50,51). DAT is amenable to regulation via presynaptic
105 receptors, either directly or via G proteins, membrane lipids and protein kinases that mediate receptor
106 signaling effects (42,51–54). For example, DA D_2-type autoreceptors (D2ARs) directly interact with DAT
107 and activation of D2ARs has been shown to promote increased DAT surface trafficking (52,55) via an
108 Extracellular signal-Regulated Kinases 1 and 2 (ERK1/2)-dependent mechanism (52). Notably, as a result
109 of DAT Val559-associated ADE, tonic stimulation of presynaptic D2ARs recruits efflux prone DAT Val559
110 to the cell surface (56) resulting in a positive feedback-loop that maintains high levels of DAT-dependent
111 ADE. Previously, we demonstrated that D2AR-mediated regulation of DAT in male mice is circuit-specific,
112 as this regulation is seen in nigrostriatal DA projections to the dorsal striatum (DS) but not the
113 mesoaccumbal projections to the ventral striatum (VS) (56). Strikingly, we recently found that the circuit
114 specificity of presynaptic D2AR regulation of DAT is also remarkably sex-specific, with an opposite
115 anatomical pattern of D2AR-DAT coupling seen in female mice, leading to enhanced DAT Val559 surface
116 trafficking in the VS, but not in the DS, a difference that we theorize may contribute to the sex-specific
117 changes observed in multiple DA-linked disorders (24).
118

119 Targeting DAT to reduce ADE, as with psychostimulants, invokes use of agents with significant abuse
120 liability (57). Thus, we sought an alternative path for DAT modulation that might normalize DAT Val559
121 phenotypes with lesser side-effects. In this regard, converging evidence has established a link between
122 kappa opioid receptor (KOR) signaling and functional regulation of DA neurotransmission. For example,
123 KORs are expressed in DA neurons (58) and KOR agonists directly inhibit DA neuron activity (59), which is
124 believed to contribute to stress-related dysphoria (60), resulting from increased secretion of the
125 endogenous KOR ligand dynorphin during stressful events. In addition, exposure to KOR agonists
126 promotes an increase in DAT-mediated DA uptake by increasing DAT surface-trafficking(54). Importantly,
127 KOR antagonism has been found to be well-tolerated in humans (61–65) suggesting opportunities to
128 modulate DA signaling therapeutically via these agents. As a test of this idea, we explored whether KOR
129 signaling can mimic or offset the biochemical and behavioral disruptions observed in DAT Val559 mice. In
130 our current report, using transfected cells and native tissue preparations, we found that activation of KOR
131 increases DAT surface trafficking and DAT N-terminal phosphorylation at threonine 53 (Thr53), a site
132 linked to DAT functional regulation and psychostimulant effects (22,66). Conversely, we found that KOR
133 antagonism reduced basal hyperphosphorylation of DAT Thr53 and surface trafficking observed in male
134 DAT Val559 DS and restored normal rates of activity-dependent vesicular DA release in this model. Finally,
135 KOR antagonism normalized sex-dependent, DAT Val559-induced perturbations in cognitive and
136 locomotor behavior.

137 **Materials and Methods**

138 Detailed Methods are provided as Supplemental Information (SI)

139

140 *Materials*

141 Lipofectamine™ 2000, Dulbecco's Modified Eagle Medium (DMEM) and other cell culture media were
142 purchased from Invitrogen/Life Technologies, (Grand Island, NY). [^{3}H]DA (dihydroxyphenylethylamine
143 [2,5,6,7,8-3H], 63.2 Ci/mmol) and Optiphase Supermix, were purchased from PerkinElmer Inc., (Waltham,
144 MA, USA). U69,593, U0126, protease and phosphatase cocktails were obtained from Sigma-Aldrich (St.
145 Louis, MO). Nor-binaltorphimine dihydrochloride (norBNI) was purchased from Tocris (Bristol, United
146 Kingdom). Reagents for SDS-polyacrylamide gel electrophoresis and Bradford protein assays were from
147 Bio-Rad (Hercules, CA, USA), fetal bovine serum and enhanced chemiluminescence (ECL) reagents were
148 from Thermo Fisher Scientific Inc., (Rockford, IL, USA). Sulfosuccinimidyl-2-[biotinamido] ethyi-1,3-
149 dithiopropionate (EZ link NHS-Sulfo-SS-biotin), Protein A magnetic beads (Dynabeads) and NeutrAvidin
150 Agarose were purchased from Thermo Scientific (Waltham, MA, USA). Anti-Calnexin antibody (Cat# ADI-
151 SPA-860-D, RRID: AB-10616095) was obtained from Enzo Life Sciences, Inc (Farmingdale, NY, USA).
152 QuikChange II XL site-directed mutagenesis kit was obtained from Agilent Technologies (Santa Clara, CA,
153 USA). Peroxidase-affinipure goat anti-rabbit IgG antibody (HRP conjugated secondary antibody (Cat# 111-
154 035-003, RRID: AB-2313567) was acquired from Jackson Immuno Research Laboratories (West Grove, PA).
155 DAT antibody Cat# 431-DATC, RRID: AB-2492076 – was used for experiments using EM4 cells. DAT
156 antibody MAB369 (Millipore Sigma, RRID:AB_2190413) -was used for experiments using acute slices). DAT
157 antibody MABN669 (Millipore Sigma, RRID:AB_2717269) was used for experiments in rat striatal
158 synaptosomes. DAT Thr53 antibody p435-53 (PhosphoSolutions, RRID: AB-2492078) was used to detect
159 DAT phosphorylated at Thr53 in all experiments.

160

161 *Cell culture, transfection of DAT cDNAs, and [3H]DA uptake assays*

162 EM4 cells were cultivated as described previously (54). Cells were co-transfected with cDNA constructs
163 encoding myc-KOR plus rDAT-WT, or myc-KOR plus rDAT Ala53, or myc-KOR plus pcDNA3 using
164 Lipofectamine 2000 24 hrs prior to the assay. QuikChange II XL site-directed mutagenesis kit was used to
165 alter rat DAT cDNA sequence encoding threonine at amino acid 53 (Thr53) to encode alanine (Ala53).
166 Uptake of [^{3}H]DA into EM4 cells co-transfected with cDNA constructs containing KOR plus rDAT, or rDAT
167 Ala53, or pcDNA3 was assessed following established methods as previously described(54).

168

169 *EM4 cell surface biotinylation*

170 Cell surface biotinylation was performed as described previously (54). In brief, transfected EM4 cells were
171 exposed to either vehicle or U69,593 (10 µM) for 30 min at 37°C. Following biotinylation of surface
172 proteins on ice for 30 min, labeled proteins were recovered after cell solubilization using Neutravidin
173 Agaraose resins. Eluates, aliquots of total extracts and unbound fractions were used for SDS-PAGE and
174 immunoblot analysis as described in the SI.

175

176 *Animals*

177 All procedures involving animals were approved by the Institutional Animal Care and Use Committees of
178 UT San Antonio Health Sciences Center, Virginia Commonwealth University, or Florida Atlantic University
179 depending on the site of assays, in accordance with the National Institutes of Health Guide for the Care
180 and Use of Laboratory Animals. Male Sprague-Dawley rats (175-350 g body weight) were utilized for *in*
181 *vivo* chronoamperometry and assays of DAT Thr53 phosphorylation in synaptosomes and tissue. For slice
182 experiments, age-matched 4- to 6-week-old male homozygous mice for either WT or DAT Val559 (genetic
183 background: 75% 129/6 and 25% C57; (18)) were bred from homozygous dams and sires that were derived
184 from heterozygous breeders. Male mice were used for experiments performed in acute slices due to the
185 male bias observed in ADHD diagnosis (67). All biochemical experiments were conducted during the light
186 phase. For behavioral experiments, 6–8-week-old WT and homozygous DAT Val559 littermates derived
187 from heterozygous breeders were utilized. Male mice were used for all behavioral experiments except
188 the novel object recognition test due to the demonstrated sex bias of behavioral phenotypes observed in
189 DAT Val559 mice (24). Behavioral testing was performed during the dark phase of the light cycle under
190 red light. Rodents were maintained in a temperature and humidity-controlled room on a 12:12 h
191 light/dark cycle. Food and water were supplied *ad libitum*. All efforts and care were taken to minimize
192 animal suffering and to reduce the number of animals used. As alternatives to brain tissues, cell culture
193 models were utilized.

194

195 *Treatment of striatal synaptosomes with U69,593 ± U0126*

196 Male Sprague-Dawley rats (175–300 g) were decapitated, and striata were rapidly dissected, weighed,
197 and placed in ice-cold sucrose phosphate (SP) buffer (0.32 M sucrose and 10 mm sodium phosphate, pH
198 7.4). Tissues were homogenized in ice-cold SP buffer with 15 strokes in a glass/Teflon homogenizer and
199 centrifuged at 3000 × *g* for 3 min at 4 °C. Supernatant fractions were re-centrifuged at 17,000 × *g* for 12
200 min, and the resulting P2 pellet enriched for synaptosomes was resuspended to 20 mg/mL original wet

201 weight in ice-cold SP buffer. Synaptosomes were treated with vehicle or 50 µM U0126 for 15 min at 30˚C,
202 followed by treatment with vehicle or 10 µM U69,593 for an additional 15 min at 30˚C. After treatment,
203 samples were subjected to SDS-PAGE followed by immunoblotting for total DAT and DAT phosphorylated
204 at Thr53).
205
206 *p-Thr53 DAT levels from rats injected with vehicle or U69,593*
207 Male rats were injected s.c. with vehicle or 0.32 mg/kg U69,593 and sacrificed at the indicated times noted
208 in Figure 3. DS or VS were dissected, weighed and kept frozen until analyzed. The pre-weighed samples
209 were homogenized with a Polytron PT1200 homogenizer (Kinematica, Basel, Switzerland) for 8 s in ice-
210 cold SP buffer, and centrifuged at 3000 × *g* for 3 min at 4 °C. Supernatant fractions were re-centrifuged at
211 17,000 × *g* for 12 min to obtain a membrane pellet. The pellet was resuspended to 20 mg/mL original wet
212 weight in ice-cold SP buffer. Samples were subjected in duplicate to SDS-PAGE and western blot for total
213 and p-Thr53 DAT, and p-Thr53 DAT staining quantified by normalization to the time-matched controls.
214
215 *Analysis of in vivo DA clearance in NAc*
216 High-Speed *in vivo* chronoamperometry, conducted as previously described (68), was used to determine
217 the effect of KOR modulators on DA clearance in NAc of anesthetized rats. Briefly, carbon fiber electrodes
218 were attached to multi-barrel glass micropipettes. Rats were anesthetized with chloralose (85 mg/kg, i.p.)
219 and urethane (850 mg/kg, i.p). Electrodes were lowered into the NAc (69)using a stereotaxic frame.
220 Individual micropipette barrels were filled with DA (200 µM), U69,593 (885.7 µM, barrel concentration),
221 norBNI (400 µM, barrel concentration) and vehicle and ejected (100–150 nL) using a Picospritzer II
222 (General Valve Corporation, Fairfield, NJ)(68). DA was pressure-ejected until a stable baseline signal was
223 established (typically after 3-4 ejections). The effect of U69,593, norBNI, and vehicle on DA signals was
224 quantified 2 min after a stable baseline DA signal was established. See SI for experimental details.
225
226 *Surface biotinylation and immunoprecipitation of p-Thr53 DAT using acute mouse brain slices*(56)
227 *Acute slice preparation:* 300 µm thick acute coronal slices were prepared from 4-6 week-old male mice.
228 Following recovery, plane-matched hemi slices were exposed to either vehicle or drug (U69,593: 10 µM
229 for7 min. norBNI: 1 µM for 20 min) at 37 °C . After drug treatments, the slices were subjected to three
230 rapid washes and two 5-min washes on ice. For immunoprecipitation studies, VS and DS were dissected
231 at this point and tissue was flash frozen in liquid nitrogen and stored at -80 °C until processed. For
232 biotinylation assays, the slices were exposed to 1 mg/mL EZ link NHS-Sulfo-SS-biotin for 30 min on ice with

233 constant oxygenation. Following washes, tissue was solubilized in RIPA buffer and biotinylated preoteins
234 were recovered using Streptavidin Agarose beads. The experimental procedures for the biotinylation and
235 immunoprecipitation assays are described in detail in (56) and in the SI.
236
237 *Behavioral testing*
238 Y Maze, Open Field test, cocaine-induced locomotor activation, and the novel object recognition (NOR)
239 test were performed using 6-8 week old male and female (only for the NOR test) mice in the Stiles-
240 Nicholson Brain Institute Neurobehavior Core of Florida Atlantic University based on established protocols
241 (24) and are described in detail in the SI.
242
243 *In vivo microdialysis*
244 Microdialysis was performed using 6–8-week-old male mice. Surgeries to insert microdialysis guide
245 cannulae were performed as described earlier (18,69). A 5 mm guide cannula was lowered into the DS
246 and affixed to the skull with dental cement, supported by three 1.6 mm screw. Mice were allowed to
247 recover for 6 days. 12 hr prior to the experiment a microdialysis probe with an active membrane length
248 of 3 mm was inserted into the guide cannula and microdialysis, sample collection and analsyis were
249 performed as described in (18). After collection of the three baseline fractions, mice received an i.p.
250 injection of norBNI (10 mg/kg) and cocaine hydrochloride (10 mg/kg; i.p.) was injected 80 min thereafter.
251 Changes in extracellular DA were expressed as fold increase of basal DA (i.e. the average DA of the first
252 three basal dialysates).
253
254 *Statistical analyses*
255 Prism 7 (GraphPad, San Diego, CA) was used for data analysis and graph preparation. Values are presented
256 as mean ± standard deviation (SD). One-way or two-way ANOVA were used followed by post hoc testing
257 for multiple comparisons. The type and results of post hoc tests are noted in the Figure legends. Two-
258 tailed, unpaired Student's t-tests were performed for comparisons between two groups. P values ≤ 0.05
259 were considered statistically significant.
260
261 *Data Availability*
262 All data will be provided by the corresponding authors upon request.
263

264 **Results**

265 *KOR regulation of DAT activity requires the capacity to phosphorylate DAT at N-terminal residue Thr53.*

266 To initiate our evaluation of KOR manipulation as a strategy for offsetting DAT-dependent alterations in
267 DA homeostasis, we transiently transfected EM4 cells with rat cDNAs encoding KOR and DAT (rKOR and
268 rDAT, respectively). In agreement with a previous study (54), activation of KOR enhanced DAT-mediated
269 uptake in a time and concentration dependent manner (Figure 1 A, B). We selected 10 µM U69,593 and a
270 15 min pre-treatment for subsequent *in vitro* experiments and found that exposure to U69,593
271 significantly increased DA transport V_{max} (336.1 ± 18.12 (SD) versus 551.2 ± 21.79 (SD) pmol/min/10^6 cells),
272 whereas DA K_M was unaffected (Figure 1C).

273

274 The site(s) or motifs in DAT through which KOR regulates DAT function have not been defined.
275 Comprehensive research has identified DAT phosphorylation as a key mechanism that determines DAT
276 activity and membrane trafficking (51,70,71). We focused on the N-terminus due to evidence that the
277 MAP kinase ERK1/2 supports KOR regulation of DAT (54) and a conserved, N-terminal proline-directed
278 kinase consensus phosphorylation motif containing Thr53 that can be phosphorylated in *vitro* by ERK1
279 (72) has been implicated in DAT function *in vitro* and *in vivo* (66,73,74). We first generated two truncated
280 versions of rDAT, lacking either the first 22 (Δ1-22) or 55 (Δ1-55) N-terminal residues. Despite the loss of
281 multiple phosphorylation sites that are found within the most distal N-terminus (51,71), rDAT Δ1-22
282 remained amenable to regulation via activation of rKOR, as treatment with U69,593 significantly increased
283 DA uptake in EM4 cells coexpressing rDAT ΔN1-22 and rKOR (Figure 1D). In contrast, no uptake stimulation
284 by U69,593 was evident in cells transfected with rKOR and rDAT ΔN1-55. Given that Thr53 is located in
285 the region that distinguishes ΔN1-55 from Δ1-22, we replaced Thr53 with an alanine (rDAT Ala53) to
286 preclude phosphorylation at this site. Single point and saturation uptake analyses in EM4 cells transfected
287 with rKOR and either WT rDAT or rDAT Ala53 revealed an absolute requirement for Thr53 phosphorylation
288 potential for U69,593 to increase DA uptake (Figure 1E-F). Saturation analysis also demonstrated that a
289 reduction in V_{max} supports the basal reduction in rDAT Ala53 DA uptake (124.4 ± 18.45 (SD)
290 pmol/min/10^6cells)) evident in comparison to WT rDAT (337.4 ± 57.65 (SD) pmol/min/10^6cells) (Figures
291 1C, 1F).

292

293 *KOR agonism increases rDAT surface levels in a Thr53-dependent manner in EM4 cells*

294 Given the well-established relationship between DAT surface expression and DA uptake, we next sought
295 to determine whether the Thr53-dependent KOR elevation of rDAT-mediated uptake correlates with an

296 increase in transporter surface expression. To pursue this objective, we biotinylated transfected cells with
297 the membrane-impermeant reagent EZ link NHS-Sulfo-SS-biotin and recovered biotinylated surface
298 proteins from total protein extracts. Exposure of cells to U69,593 had no effect on total levels of either
299 WT rDAT or rDAT Ala53 (Figure 2A). Western blots of total extracts revealed WT rDAT to migrate as distinct
300 bands of ~55-60 kDa and ~85-90 kDa, typical of rDAT transiently transfected cells and linked to different
301 transporter species bearing mature versus immature states of N-glycosylation (75). In contrast to the WT
302 rDAT protein profile, extracts from cells expressing the DAT Ala53 mutant were depleted of the 85-90 kDA
303 species. Analysis of rDAT species in biotinylated samples showed that U69,593 significantly increased WT
304 rDAT surface density for both the ~55-60 kDa and ~85-90 kDa DAT bands. In contrast, neither species of
305 rDAT Ala53 was affected by U69,593 treatment (Figure 2B). To detect rDAT Thr53 phosphorylation (p-
306 Thr53), we probed blots with a DAT p-Thr53 specific antibody (66). We found that U69,593 treatment
307 significantly increased immunoreactivity for the ~85-90 kDa isoform of DAT p-Thr53 labelled proteins in
308 total extracts from WT rDAT transfected cells, whereas increased DAT p-Thr53 labelling of the WT rDAT
309 ~55-60 kDa isoform was not detected. Importantly, no DAT-specific bands of either isoform were detected
310 in surface-samples from cells transfected with the rDAT Ala53 variant (Figure 2C). Finally, when we
311 analysed blots from extracts recovered after surface biotinylation, we detected a significant increase in
312 DAT p-Thr53 immunoreactivity for both isoforms of WT DAT, whereas no DAT p-Thr53-specific bands were
313 detected in the case of the Ala53 variant (Figure 2D). Of note, the DAT p-Thr53 antibody detected some
314 non-specific bands, which were also present in mock-transfected cells (* in Figures 2C and D) and
315 therefore not considered for analysis. Together, our findings indicate that capacity for Thr53
316 phosphorylation is essential for enhanced surface trafficking of rDAT in response to rKOR agonism in EM4
317 cells.
318
319 *Pharmacological activation of KOR increases rDAT phosphorylation at Thr53 in striatal synaptosomes and*
320 *enhances DA clearance in vivo*
321 Having established in transfected cells that a capacity for rDAT Thr53 phosphorylation plays an essential
322 role in KOR-dependent elevations of transporter surface trafficking and DA uptake, we next sought to
323 determine whether these findings could be replicated in native tissue. As shown in Figure 3A, treatment
324 of rat striatal synaptosomes with U69,593 promoted a significant increase in p-Thr53 DAT
325 immunoreactivity that could be blocked by inhibition of mitogen-activated protein kinase kinase (MEK1/2)
326 using U0216, which lies upstream of ERK 1/2 (Figure 3A). To assess whether KOR activation can elevate p-
327 Thr53 DAT *in vivo*, male rats were injected with U69,593 (0.32 mg/kg, i.p.) or vehicle and sacrificed at the

328 time points shown in Figure 3B and C. To parse out whether circuit-specific effects that shape the outcome
329 of D2AR regulation of DAT surface trafficking (24,56) also exist for KOR, we analysed the impact of
330 systemic U69,593 on p-Thr53 DAT by western blot in both the DS (Figure 3B) and VS (Figure 3C). For both
331 DS and VS, systemic U69,593 caused a time-dependent increase in p-Thr53 DAT that peaked at 120min
332 post injection. Considering the effects of KOR activation to increase DAT-mediated DA uptake in cells
333 (Figure 1 and (54)), we sought *in vivo* evidence for increased DAT function following KOR activation via
334 assessment of DA clearance time using high-speed *in vivo* chronoamperometry (68,76). A carbon fiber
335 electrode-micropipette assembly was lowered into the NAc (Figure 3D) permitting DA to be pressure
336 ejected, followed by recording of DA levels as a function of time. Representative traces depicting DA
337 clearance before and after administration of U69,593 are shown in Figure 3E. We found that local injection
338 of U69,593 decreased DA clearance time compared to predrug baseline, quantified as the time required
339 to clear 50% (T50) and 80 % (T80) of the DA-induced amperometric signal (Figure 3F). In contrast, pre-
340 treatment with the KOR antagonist norBNI significantly increased clearance time consistent with a non-
341 saturating level of endogenous KOR activation under our recording conditions (Suppl. Figure 2).
342
343 *Targeting KOR to normalize aberrant surface trafficking and phosphorylation of the disease associated*
344 *DAT variant Val559 in vivo*
345 DAT Val559 expression in male mice is associated with increased surface trafficking of DAT and elevated
346 levels of p-Thr53 DAT in the DS but not the VS (56). The ability of KORs to regulate DAT via phosphorylation
347 of Thr53 raised the possibility that pharmacological antagonism of mKORs might normalize the tonically
348 elevated surface expression of efflux-prone mDAT Val559 proteins. To determine whether mDAT Val559
349 remains amenable to regulation via mKOR in native brain preparations, we first treated acute coronal
350 slices containing either DS or VS of WT mDAT or mDAT Val559 *in vitro* with U69,593 (10 µM, 7 min),
351 extracting DAT proteins thereafter for analysis of transporter surface trafficking and p-Thr53 levels via
352 western blots. *In vitro* activation of mKOR increased surface trafficking of DAT independent of genotype
353 in both the DS (Figure 4A) and VS (Figure 4C). As with surface transporter density, and as previously
354 reported (56), blots of mDAT Val559 extracts from male DS (Figure 4B) but not VS (Figure 4D),
355 demonstrated significantly elevated levels of p-Thr53 DAT relative to WT mDAT under vehicle-treated
356 conditions. Whereas U69,593 (10 µM, 7 min) increased levels of p-Thr53 DAT in extracts both from DS
357 (Figure 4B) and VS (Figure 4D) of WT male mice as well as VS from DAT Val559 male mice (Figure 4 D), this
358 effect was blunted in male DAT Val559 preparations from the DS (Figure 4).

359 We found that norBNI (1 µM, 20 min) produced no effect on either surface density or DAT p-Thr53 levels
360 when applied to WT DAT DS slices. However, treatment with norBNI in vitro normalized the elevations
361 observed in both transporter surface density (Figure 4E) and p-Thr53 DAT (Figure 4F) in the DS of DAT
362 Val559 mice relative to WT controls. In the VS, norBNI was without effect on transporter trafficking or p-
363 Thr53 levels of either WT or DAT Val559 mice (Figure 4 G and H). To establish that this effect is of relevance
364 in vivo, we treated pairs of WT and DAT Val559 mice either with saline or norBNI (10 mg/kg, i.p.) 30 min
365 prior to the collection of acute coronal slices, which were then subjected to immediate surface
366 biotinylation. Enhanced surface expression of mDAT Val559 relative to WT mDAT was evident in slices
367 prepared from saline treated animals, whereas no difference in surface density was observed following
368 norBNI treatment (Supplementary Fig 3).
369
370 *In vivo KOR antagonism rescues vesicular DA release and behavioral deficits in DAT Val559 mice*
371 Consistent with tonic D2AR activation and D2AR-mediated suppression of vesicular DA release, *ex vivo*
372 studies with striatal slices from male DAT Val559 mice revealed a significant reduction of evoked vesicular
373 release of DA (18). Additionally, *in vivo* microdialysis in the DS of these animals revealed a loss of cocaine
374 (10 mg/kg, i.p.) induced elevations in extracellular DA (20). We hypothesized that mKOR inhibition, due
375 to its ability to reduce the elevated basal surface trafficking of efflux-prone mDAT Val559 should restore
376 vesicular DA release in vivo. Indeed, as assed by in vivo microdialysis, when male mice were treated with
377 norBNI (10 mg/kg; i.p.) 80 min prior to an i.p. injection of cocaine (10 mg/kg), we found that cocaine now
378 evoked a robust increase in extracellular DA in DAT Val559 mice, equivalent to that seen with WT mice
379 (Supplementary Figure 4 A-C).
380
381 To determine whether a restoration of vesicular DA release might lead to a normalization of behaviors
382 found to be disrupted in male and female DAT Val559 mice. First, we chose the Y-maze test of
383 spontaneous alternation, a measure whose reduction is considered a symptom of disrupted working
384 memory or compulsive repetitive behavior. Male but not female DAT Val559 mice display a robust
385 reduction in alternations in the Y maze, when compared to WT littermates, driven by immediate return
386 to a previously visited arm (direct revisits) (Figure 5A through D and (24)) that was not explained by
387 changes in locomotor activity (Figure 5C and (24)). Strikingly, an acute injection of norBNI (10 mg/kg, i.p.
388 30 min prior to initial Y maze testing) normalized the alternation deficit of DAT Val559 mice (Figure 5B) as
389 well as the direct revisits monitored in the task (Figure 5D) without an effect on locomotor behavior
390 (Figure 5 C).

391 DAT Val559 affects DA circuits in a sex-dependent manner that leads to distinct behavioral outcomes in
392 males versus females (24). To determine if systemic treatment with norBNI (10 mg/kg, i.p.) is also capable
393 of reversing a female-specific phenotype of DAT Val559 expression, we implemented the novel object
394 recognition (NOR) test, where female but not male DAT Val559 mice display strong differences in novel
395 object preference and discrimination, as female DAT Val559 mice do not explore a novel object to the
396 same extent as WT controls (24). Again, treatment with norBNI (10 mg/kg, i.p.) restored the discrimination
397 index and time spent with the novel object of female DAT Val559 mice to levels that were comparable to
398 those observed in female WT mice (Figure 5E through J). Importantly, deficits in the relative interaction
399 time and discrimination index are not confounded by locomotor activity or total object interaction time
400 on testing day 1 or testing day 2 (Figure 5 F,G,H,I and J, respectively), as all these measures remained
401 unchanged in female DAT Val559 mice. Consequently, these findings demonstrate that mKOR antagonism
402 can normalize behavioral changes unique to either male or female DAT Val559 mice.
403
404 NorBNI is associated with long lasting effects *in vivo* (77,78). Therefore, we reassessed Y maze activity in
405 the same male experimental subjects as reported above, one week after the initial test. One week
406 following the initial study, the vehicle treated male DAT Val559 mice continued to display a deficit in
407 alternations (Supplementary Figure 5B) that was not driven by altered locomotor activity (Supplementary
408 Figure 5C) but rather the result of an increase in direct revisits when compared to WT controls
409 (Supplementary Figure 5D).In contrast, the norBNI treated DAT Val559 mice displayed a significantly
410 altered alternation pattern when compared to vehicle treated DAT Val559 mice (Supplementary Figure
411 5B). Moreover, the norBNI treated DAT Val559 group exhibited a direct revisit pattern that was statistically
412 indistinguishable from vehicle treated WT controls (Supplementary Figure 5D), whereas no drug or
413 genotype effect on total distance travelled during the Y maze test sessions was observed one week post
414 norBNI treatment (Supplementary Figure 5C).
415
416 We further examined the behavior of the vehicle and norBNI treated cohorts one week post
417 administration in the open field test (OFT). Unlike DAT KO mice (12), male (or female) DAT Val559 mice
418 are not spontaneously hyperactive, though male DAT Val559 mice display increased locomotor reactivity
419 (darting) in response to imminent handling (18). In the OFT, male DAT Val559 mice displayed locomotor
420 suppression (distance travelled, rearing and stereotypy), as compared to WT littermates (Figure 6A,B).
421 Remarkably, injection of norBNI 7 days prior to testing normalized these measures (Figure 6D,E). We
422 hypothesize that the reduced locomotion of the saline treated DAT Val559 mice may represent

423 heightened anxiety post handling, since DAT Val559 mice demonstrated reduced center time in the open
424 field (Fig 6C), a behavioral measure known to be responsive to anxiolytics (79). Systemic norBNI also
425 normalized this measure (Figure 6C). DAT Val559 further mice display a blunted locomotor response to
426 psychostimulants, including cocaine (10 mg/kg, i.p.) (18,20). Pretreatment with norBNI (10 mg/kg, i.p.)
427 one week prior to testing restored the locomotor response of male DAT Val559 mice to systemic cocaine.
428 In the norBNI treated group, the increase in cocaine-induced locomotor activity was concomitant with an
429 increase in time spent in the center of the chamber, with the latter measure being absent in saline treated
430 controls (Figure 6 F and G).

431 **Discussion**

432 Dysfunction in DAergic signaling has been linked to multiple neuropsychiatric disorders including ADHD
433 (80), schizophrenia (81) and ASD (82). Initial efforts to model disturbed DA-signaling primarily aimed to
434 disrupt vesicular release (83), reuptake (12) or synthesis of DA (84) using knock-out animals. The DAT
435 knock-out model suffers, however, from issues related to construct validity with respect to most DA-linked
436 neurobehavioral disorders as homozygous loss-of-function DAT mutations in humans exhibit Juvenile
437 Dystonia/Parkinsonism and require intensive support to live past early childhood (85,86). In the current
438 study, we utilized mice expressing DAT Val559, an extensively characterized disease associated variant of
439 the DAT (87), as a platform to search for a pharmacological manipulation that could normalize biochemical
440 and behavioral traits seen with genetic DAT dysfunction. Specifically, based on considerations of the ability
441 of KORs to regulate presynaptic mechanisms in both nigrostriatal and mesolimbic DA neurons (88,89) and
442 recently published clinical evidence demonstrating that KOR-antagonism is well-tolerated in humans (61–
443 65), we explored whether antagonism of KOR-mediated regulation of DAT might display therapeutic
444 potential for the treatment of DA-linked disorders.

445

446 We report that activation of KOR enhances DAT-mediated uptake by promoting an increase in surface
447 DAT, consistent with a previous study (54), though the prior work did not explore the post-translational
448 modifications and motif(s)/site(s) through which KOR regulates DAT surface expression. We found that
449 mutation of the canonical ERK1/2 site Thr53 to Ala53 prevented the KOR agonist U69,593 from inducing
450 elevations in DA transport V_{max}, DAT surface expression and phosphorylation of Thr53 DAT, providing
451 evidence that KOR-mediated regulation of DAT is contingent on Thr53 (Figures 1 and 2).

452 Enhanced DAT surface expression in acute brain slices, paralleled by elevated phosphorylation at Thr53,
453 was evident in WT VS and DS slice preparations following KOR-agonist exposure (Figure 4). Moreover,
454 high-speed chronoamperometry in live animals revealed that while the KOR-agonist U69,593 accelerated
455 DA clearance, the KOR-antagonist norBNI prolonged DA clearance from the extracellular space (Figure 3),
456 establishing for the first time the dependence of *in vivo* DA clearance on endogenous KOR signaling and
457 consistent with a link of Thr53 phosphorylation to both KOR regulated trafficking and increased DA
458 clearance capacity. We have previously demonstrated that D2AR-mediated regulation of DAT is sex and
459 region specific, which results in elevated DAT Val559 surface expression and Thr53 hyperphosphorylation
460 in the DS of males (56) and VS of females (24). However, no region-specificity was observed for KOR in
461 this regard (Figure 4) Interestingly, treatment with U69,593 significantly elevated surface DAT Val559 in
462 the DS, without promoting a further increase in phosphorylation at Thr53 (Figure 4), which contrasts with

463 our experiments in EM4 cells (Figure 2). This might indicate that phosphorylation at Thr53 reached a
464 ceiling effect in the DS of DAT Val559 mice and that KOR can recruit additional and/or unknown regulatory
465 mechanisms in native tissue preparations that are absent in heterologous expression systems. Using acute
466 brain slices, we found that treatment with norBNI normalized the aberrant surface trafficking and
467 hyperphosphorylation at Thr53 of DAT Val559 in the DS (56).
468
469 Mergy and colleagues have shown that expression of DAT Val559 dampens the vesicular release of DA,
470 due to tonic stimulation of inhibitory D2ARs (18). Consequently, administration of the non-selective DAT
471 inhibitor cocaine fails to elevate extracellular DA in the DS of male Val559 mice (20). We found that pre-
472 treatment with norBNI fully restored the DA response to cocaine in male mice (Figure 6 and
473 Supplementary Figure 4). This finding supports the interpretation that inhibition of KOR and subsequent
474 normalization of surface trafficking of DAT Val559 aids in restoration of vesicular DA release in DAT Val559
475 mice. Additional studies are needed to clarify the contribution of somatic KOR versus presynaptic KOR in
476 the ability of KOR antagonists to restore vesicular DA despite elevated D2AR signaling. Mice are available
477 that lack KOR in DAergic neurons (90). Future studies with such animals should help define whether the
478 effect of norBNI in DAT Val559 mice exclusively relies on its action at KORs expressed on DA synthesizing
479 neurons versus other sites. Similarly, additional approaches are needed to identify the source(s) of
480 dynorphin that allow for the ability of KOR to normalize traits in DAT Val559 mice. While a striatal source
481 of dynorphin that could account for modulation of DAT Val559 by KORs has been documented (12), we
482 have demonstrated that a serotonergic plasticity arises in DAT Val559 mice that drives a loss of locomotor
483 activation by cocaine (20). In this regard, Pomrenze et al (91) have recently demonstrated that
484 serotonergic projections to the NAc produce and release dynorphin and are worth exploring.
485
486 At present, we cannot exclude the possibility that treatment with norBNI reduces DAT Val559-mediated
487 reverse transport *per se* as well as surface expression. DAT Val559 is hyperphosphorylated at DAT N-
488 terminal sites that have been linked to reverse transport (42,66). Antagonism of KOR normalized the
489 hyperphosphorylation at Thr53 and this observation could expand to other phosphorylation sites crucial
490 for reverse transport. Further, Lycas et al (92) reported that activation of D2ARs causes DAT to accumulate
491 in nanoclusters in which DAT appears to be biased towards the inward facing conformation. The authors
492 found that another disease-assciated efflux-prone DAT variant (DAT-Asp421Asn) that is conformationally
493 biased towards the inward-facing conformation preferentially localized to these clusters. Considering the
494 tonic activation of D2ARs, DAT Val559 may reside in nanodomains that support ADE in DAergic neurons

495 whereas antagonism of KOR could redistribute DAT Val559 into nano-environments that preclude ADE.
496 Alternatively, antagonism of KOR could further disrupt the potentially enhanced interaction of DAT Val559
497 with proteins and lipids that bias DAT towards more efflux-prone states (49,93–96). Activated Gbg
498 proteins have also been found to induce DA efflux similar to that seen with DAT Val559 and amphetamines
499 (44,45). Whether the pathways involved with KOR antagonism intersect with this mechanism and its
500 regulators are worthy of study. More generally, such considerations suggest that DAT mutations are likely
501 only one mechanism by which behaviorally penetrant DA efflux states can arise, and where KOR
502 antagonism can be of therapeutic use.
503
504 On a behavioral level, male DAT Val559 mice display a deficit in spontaneous alternation in the Y-Maze
505 test ((24)and Figure 5), which translates into deficits in working memory (97). Administration of norBNI
506 normalized the deficit in spontaneous alternations and direct revisits 30 min and one week post injection.
507 The latter observation is consistent with the long-lasting effects of norBNI (77,78). Of note, a recent study
508 demonstrated that norBNI improved working memory and attention in the perinatal nicotine exposure
509 model, presumably via an increase in cortical DA (98). Prenatal exposure to nicotine alters development
510 of the DA system and direct effects of this paradigm on DAT have been reported (99). Moreover, nicotinic
511 acetylcholine receptors are well known to regulate DA vesicular release (100). This suggests that the
512 beneficial effect of norBNI could arise from normalization of disrupted presynaptic signaling networks that
513 dictate DA release and clearance. Future studies assessing DA dynamics in WT and DAT Val559 in mPFC,
514 VS and DS in the context of DAT, D2AR and KOR antagonists directly administered in these regions are
515 underway to tease apart the relative contribution of the respective terminal fields of DA neurons
516 emanating from VTA and SNc.
517
518 In line with the persistent effect of norBNI in the Y-Maze, we also found that norBNI normalized behavior
519 of male DAT Val559 mice in the open field one week after norBNI administration. Vehicle treated DAT
520 Val559 mice spent significantly less time in the center than WT controls and this difference was absent
521 when mice were treated with norBNI prior to testing (Figure 6), consistent with an anxiolytic effect.
522 Interestingly, we (18) found no differences in horizontal locomotor activity between WT and DAT Val559
523 mice in the open field. The reduction in horizontal locomotor activity of male Val559 DAT mice observed
524 in this study (Figure 6) might be attributed to repeated handling and an increased susceptibility of these
525 mice to repeated stress. We also observed that saline treated DAT Val559 mice displayed a reduced
526 tendency to explore the full length of the arms of the Y-Maze when they were re-exposed to the

527 apparatus. This could indicate that the exploratory behavior is suppressed in male DAT Val559 mice upon
528 repeated handling or when the novelty of the environment is removed. Moreover, pre-treatment with
529 norBNI restored the locomotor response of male DAT Val559 mice to systemic cocaine in the open field
530 (Figure 6), in agreement with re-established vesicular DA release in norBNI treated DAT Val559 mice. Of
531 note, female DAT Val559 mice display impaired performance in the NOR task and this phenotype can be
532 restored by systemic administration of the D2-antagonist sulpiride (24), in line with our interpretation
533 that behavioral deficits arise from tonic activation of D2ARs. Systemic administration of norBNI improved
534 NOR in female DAT Val559 mice (Figure 5), which suggests that antagonism of KOR rescues behavioral
535 consequences of DAT Val559 expression regardless of sex.
536
537 In conclusion, using a construct-valid preclinical model of genetic DAT dysfunction, we found that
538 inhibition of KOR normalizes aberrant biochemical and behavioral sequelae resulting from disrupted
539 DAergic neurotransmission, reinforcing the potential of KOR antagonists for the treatment of disorders
540 linked to DAT-dependent tonic DA elevation. Additionally, our findings draw attention to the interplay of
541 D2AR and KOR signaling and their regulation of DAT and DA neurotransmission under basal conditions, as
542 well augmentating vesicular DA release to achieve greater neuromodulatory DA "signal to noise".
543 Considering issues of high abuse liability with prescribing psychostimulants to treat many DA-linked
544 psychiatric pathologies, our findings support the use of a non-stimulant type medication based on KOR
545 antagonism for the treatment of DA-linked disorders where excess tonic vs phasic DA signaling is
546 suspected to underlie changes in cognitive function and/or working memory.

Acknowledgements

This work was supported by a Max Kade Fellowship of the Austrian Academy of Sciences to FPM, a NARSAD Young Investigator Grant from the BBRF to AS, P20 GM103442 to JDF, P20 GM104360 to RAV, R01 MH093320 and R21 DA046044 to LCD, R01 MH105094 to RDB and R01DA054694 to SR

Conflicts of Interest

All authors declare no conflicts of interest

554 **References**

555 1. Bromberg-Martin ES, Matsumoto M, Hikosaka O. Dopamine in Motivational Control:
556 Rewarding, Aversive, and Alerting. Vol. 68, Neuron. 2010. p. 815–34.
557 2. Berke JD. What does dopamine mean? Vol. 21, Nature Neuroscience. Nature Publishing
558 Group; 2018. p. 787–93.
559 3. Salamone JD. Complex motor and sensorimotor functions of striatal and accumbens
560 dopamine: involvement in instrumental behavior processes. Vol. 107,
561 Psychopharmacology. 1992.
562 4. Barnes JJM, Dean AJ, Nandam LS, O'Connell RG, Bellgrove MA. The molecular genetics of
563 executive function: role of monoamine system genes. Biol Psychiatry. 2011 Jun
564 15;69(12):e127-43.
565 5. Volkow ND, Wang GJ, Kollins SH, Wigal TL, Newcorn JH, Telang F, et al. Evaluating
566 Dopamine Reward Pathway in ADHD Clinical Implications [Internet]. 2009. Available
567 from: https://jamanetwork.com/
568 6. Pavăl D. A Dopamine Hypothesis of Autism Spectrum Disorder. Dev Neurosci.
569 2017;39(5):355–60.
570 7. Ashok AH, Marques TR, Jauhar S, Nour MM, Goodwin GM, Young AH, et al. The
571 dopamine hypothesis of bipolar affective disorder: the state of the art and implications
572 for treatment. Mol Psychiatry. 2017 May;22(5):666–79.
573 8. Dauer W, Przedborski S. Parkinson's disease: mechanisms and models. Neuron. 2003 Sep
574 11;39(6):889–909.
575 9. Grace AA. Dysregulation of the dopamine system in the pathophysiology of
576 schizophrenia and depression. Nat Rev Neurosci. 2016 Aug;17(8):524–32.
577 10. Russo SJ, Nestler EJ. The brain reward circuitry in mood disorders. Nat Rev Neurosci.
578 2013 Sep;14(9):609–25.
579 11. Kristensen AS, Andersen J, Jørgensen TN, Sørensen L, Eriksen J, Loland CJ, et al. SLC6
580 neurotransmitter transporters: structure, function, and regulation. Pharmacol Rev. 2011
581 Sep;63(3):585–640.
582 12. Giros B, Jaber M, Jones SR, Wightman RM, Caron MG. Hyperlocomotion and indifference
583 to cocaine and amphetamine in mice lacking the dopamine transporter. Nature. 1996
584 Feb 15;379(6566):606–12.
585 13. Jones SR, Gainetdinov RR, Jaber M, Giros B, Wightman RM, Caron MG. Profound
586 neuronal plasticity in response to inactivation of the dopamine transporter. Proc Natl
587 Acad Sci U S A. 1998 Mar 31;95(7):4029–34.
588 14. Madras BK, Miller GM, Fischman AJ. The Dopamine Transporter and Attention-
589 Deficit/Hyperactivity Disorder. Biol Psychiatry. 2005 Jun;57(11):1397–409.
590 15. Pinsonneault JK, Han DD, Burdick KE, Kataki M, Bertolino A, Malhotra AK, et al. Dopamine
591 transporter gene variant affecting expression in human brain is associated with bipolar
592 disorder. Neuropsychopharmacology. 2011 Jul;36(8):1644–55.
593 16. Heal DJ, Smith SL, Gosden J, Nutt DJ. Amphetamine, past and present--a pharmacological
594 and clinical perspective. J Psychopharmacol. 2013 Jun;27(6):479–96.
595 17. Volkow ND, Wang GJ, Fowler JS, Logan J, Franceschi D, Maynard L, et al. Relationship
596 between blockade of dopamine transporters by oral methylphenidate and the increases
597 in extracellular dopamine: therapeutic implications. Synapse. 2002 Mar 1;43(3):181–7.

598 18. Mergy MA, Gowrishankar R, Gresch PJ, Gantz SC, Williams J, Davis GL, et al. The rare DAT
599 coding variant Val559 perturbs da neuron function, changes behavior, and alters in vivo
600 responses to psychostimulants. Proc Natl Acad Sci U S A. 2014 Nov 4;111(44):E4779–88.
601 19. Davis GL, Stewart A, Stanwood GD, Gowrishankar R, Hahn MK, Blakely RD. Functional
602 coding variation in the presynaptic dopamine transporter associated with
603 neuropsychiatric disorders drives enhanced motivation and context-dependent
604 impulsivity in mice. Behavioural brain research. 2018 Jan 30;337:61–9.
605 20. Stewart A, Davis GL, Gresch PJ, Katamish RM, Peart R, Rabil MJ, et al. Serotonin
606 transporter inhibition and 5-HT2C receptor activation drive loss of cocaine-induced
607 locomotor activation in DAT Val559 mice. Neuropsychopharmacology. 2019
608 Apr;44(5):994–1006.
609 21. DiCarlo GE, Aguilar JI, Matthies HJ, Harrison FE, Bundschuh KE, West A, et al. Autism-
610 linked dopamine transporter mutation alters striatal dopamine neurotransmission and
611 dopamine-dependent behaviors. J Clin Invest. 2019 May 16;129(8):3407–19.
612 22. Ragu Varman D, Subler MA, Windle JJ, Jayanthi LD, Ramamoorthy S. Novelty-induced
613 hyperactivity and suppressed cocaine induced locomotor activation in mice lacking
614 threonine 53 phosphorylation of dopamine transporter. Behavioural brain research. 2021
615 Jun 25;408:113267.
616 23. Stewart A, Davis GL, Areal LB, Rabil MJ, Tran V, Mayer FP, et al. Male DAT Val559 Mice
617 Exhibit Compulsive Behavior under Devalued Reward Conditions Accompanied by
618 Cellular and Pharmacological Changes. Cells. 2022 Dec 15;11(24).
619 24. Stewart A, Mayer FP, Gowrishankar R, Davis GL, Areal LB, Gresch PJ, et al. Behaviorally
620 penetrant, anomalous dopamine efflux exposes sex and circuit dependent regulation of
621 dopamine transporters. Mol Psychiatry. 2022 Dec;27(12):4869–80.
622 25. Reith MEA, Kortagere S, Wiers CE, Sun H, Kurian MA, Galli A, et al. The dopamine
623 transporter gene SLC6A3: multidisease risks. Mol Psychiatry. 2022 Feb;27(2):1031–46.
624 26. Mazei-Robison MS, Couch RS, Shelton RC, Stein MA, Blakely RD. Sequence variation in
625 the human dopamine transporter gene in children with attention deficit hyperactivity
626 disorder. Neuropharmacology. 2005 Nov;49(6):724–36.
627 27. Sakrikar D, Mazei-Robison MS, Mergy MA, Richtand NW, Han Q, Hamilton PJ, et al.
628 Attention deficit/hyperactivity disorder-derived coding variation in the dopamine
629 transporter disrupts microdomain targeting and trafficking regulation. J Neurosci. 2012
630 Apr 18;32(16):5385–97.
631 28. Hansen FH, Skjørringe T, Yasmeen S, Arends N V, Sahai MA, Erreger K, et al. Missense
632 dopamine transporter mutations associate with adult parkinsonism and ADHD. J Clin
633 Invest. 2014 Jul;124(7):3107–20.
634 29. Grünhage F, Schulze TG, Müller DJ, Lanczik M, Franzek E, Albus M, et al. Systematic
635 screening for DNA sequence variation in the coding region of the human dopamine
636 transporter gene (DAT1). Mol Psychiatry. 2000 May;5(3):275–82.
637 30. Hamilton PJ, Campbell NG, Sharma S, Erreger K, Herborg Hansen F, Saunders C, et al. De
638 novo mutation in the dopamine transporter gene associates dopamine dysfunction with
639 autism spectrum disorder. Mol Psychiatry. 2013 Dec;18(12):1315–23.
640 31. de Azeredo LA, Rovaris DL, Mota NR, Polina ER, Marques FZ, Contini V, et al. Further
641 evidence for the association between a polymorphism in the promoter region of

642 SLC6A3/DAT1 and ADHD: findings from a sample of adults. Eur Arch Psychiatry Clin
643 Neurosci. 2014 Aug;264(5):401–8.
644 32. Bowton E, Saunders C, Reddy IA, Campbell NG, Hamilton PJ, Henry LK, et al. SLC6A3
645 coding variant Ala559Val found in two autism probands alters dopamine transporter
646 function and trafficking. Transl Psychiatry. 2014 Oct 14;4(10):e464.
647 33. Mazei-Robison MS, Blakely RD. Expression studies of naturally occurring human
648 dopamine transporter variants identifies a novel state of transporter inactivation
649 associated with Val382Ala. Neuropharmacology. 2005 Nov;49(6):737–49.
650 34. Herborg F, Andreassen TF, Berlin F, Loland CJ, Gether U. Neuropsychiatric disease-
651 associated genetic variants of the dopamine transporter display heterogeneous
652 molecular phenotypes. J Biol Chem. 2018 May 11;293(19):7250–62.
653 35. Bhat S, El-Kasaby A, Freissmuth M, Sucic S. Functional and Biochemical Consequences of
654 Disease Variants in Neurotransmitter Transporters: A Special Emphasis on Folding and
655 Trafficking Deficits. Pharmacol Ther. 2021 Jun;222:107785.
656 36. Leitner Y. The co-occurrence of autism and attention deficit hyperactivity disorder in
657 children - what do we know? Front Hum Neurosci. 2014;8:268.
658 37. Rommelse NNJ, Franke B, Geurts HM, Hartman CA, Buitelaar JK. Shared heritability of
659 attention-deficit/hyperactivity disorder and autism spectrum disorder. Eur Child Adolesc
660 Psychiatry. 2010 Mar;19(3):281–95.
661 38. Zhou A, Cao X, Mahaganapathy V, Azaro M, Gwin C, Wilson S, et al. Common genetic risk
662 factors in ASD and ADHD co-occurring families. Hum Genet. 2023 Feb;142(2):217–30.
663 39. Schiweck C, Arteaga-Henriquez G, Aichholzer M, Edwin Thanarajah S, Vargas-Cáceres S,
664 Matura S, et al. Comorbidity of ADHD and adult bipolar disorder: A systematic review and
665 meta-analysis. Neurosci Biobehav Rev. 2021 May;124:100–23.
666 40. van Hulzen KJE, Scholz CJ, Franke B, Ripke S, Klein M, McQuillin A, et al. Genetic Overlap
667 Between Attention-Deficit/Hyperactivity Disorder and Bipolar Disorder: Evidence From
668 Genome-wide Association Study Meta-analysis. Biol Psychiatry. 2017 Nov 1;82(9):634–
669 41.
670 41. Mazei-Robison MS, Bowton E, Holy M, Schmudermaier M, Freissmuth M, Sitte HH, et al.
671 Anomalous dopamine release associated with a human dopamine transporter coding
672 variant. J Neurosci. 2008 Jul 9;28(28):7040–6.
673 42. Bowton E, Saunders C, Erreger K, Sakrikar D, Matthies HJ, Sen N, et al. Dysregulation of
674 dopamine transporters via dopamine D2 autoreceptors triggers anomalous dopamine
675 efflux associated with attention-deficit hyperactivity disorder. J Neurosci. 2010 Apr
676 28;30(17):6048–57.
677 43. Thal LB, Tomlinson ID, Quinlan MA, Kovtun O, Blakely RD, Rosenthal SJ. Single Quantum
678 Dot Imaging Reveals PKCβ-Dependent Alterations in Membrane Diffusion and Clustering
679 of an Attention-Deficit Hyperactivity Disorder/Autism/Bipolar Disorder-Associated
680 Dopamine Transporter Variant. ACS Chem Neurosci. 2019 Jan 16;10(1):460–71.
681 44. Garcia-Olivares J, Baust T, Harris S, Hamilton P, Galli A, Amara SG, et al. Gβγ subunit
682 activation promotes dopamine efflux through the dopamine transporter. Mol Psychiatry.
683 2017 Dec;22(12):1673–9.
684 45. Pino JA, Nuñez-Vivanco G, Hidalgo G, Reyes Parada M, Khoshbouei H, Torres GE.
685 Identification of Critical Residues in the Carboxy Terminus of the Dopamine Transporter

686 Involved in the G Protein βγ-Induced Dopamine Efflux. Front Pharmacol.
687 2021;12:642881.
688 46. Mergy MA, Gowrishankar R, Davis GL, Jessen TN, Wright J, Stanwood GD, et al. Genetic
689 targeting of the amphetamine and methylphenidate-sensitive dopamine transporter: On
690 the path to an animal model of attention-deficit hyperactivity disorder. Vol. 73,
691 Neurochemistry International. Elsevier Ltd; 2014. p. 56–70.
692 47. Hong WC, Yano H, Hiranita T, Chin FT, McCurdy CR, Su TP, et al. The sigma-1 receptor
693 modulates dopamine transporter conformation and cocaine binding and may thereby
694 potentiate cocaine self-administration in rats. J Biol Chem. 2017 Jul 7;292(27):11250–61.
695 48. Egaña LA, Cuevas RA, Baust TB, Parra LA, Leak RK, Hochendoner S, et al. Physical and
696 functional interaction between the dopamine transporter and the synaptic vesicle
697 protein synaptogyrin-3. J Neurosci. 2009 Apr 8;29(14):4592–604.
698 49. Shekar A, Mabry SJ, Cheng MH, Aguilar JI, Patel S, Zanella D, et al. Syntaxin 1 Ser14
699 phosphorylation is required for nonvesicular dopamine release. Sci Adv. 2023 Jan
700 13;9(2):eadd8417.
701 50. Vaughan RA, Foster JD. Mechanisms of dopamine transporter regulation in normal and
702 disease states. Trends Pharmacol Sci. 2013 Sep;34(9):489–96.
703 51. Bermingham DP, Blakely RD. Kinase-dependent Regulation of Monoamine
704 Neurotransmitter Transporters. Pharmacol Rev. 2016 Oct;68(4):888–953.
705 52. Bolan EA, Kivell B, Jaligam V, Oz M, Jayanthi LD, Han Y, et al. D2 receptors regulate
706 dopamine transporter function via an extracellular signal-regulated kinases 1 and 2-
707 dependent and phosphoinositide 3 kinase-independent mechanism. Mol Pharmacol.
708 2007 May;71(5):1222–32.
709 53. Zapata A, Kivell B, Han Y, Javitch JA, Bolan EA, Kuraguntla D, et al. Regulation of
710 dopamine transporter function and cell surface expression by D3 dopamine receptors. J
711 Biol Chem. 2007 Dec 7;282(49):35842–54.
712 54. Kivell B, Uzelac Z, Sundaramurthy S, Rajamanickam J, Ewald A, Chefer V, et al. Salvinorin
713 A regulates dopamine transporter function via a kappa opioid receptor and ERK1/2-
714 dependent mechanism. Neuropharmacology. 2014 Nov;86:228–40.
715 55. Lee FJS, Pei L, Moszczynska A, Vukusic B, Fletcher PJ, Liu F. Dopamine transporter cell
716 surface localization facilitated by a direct interaction with the dopamine D2 receptor.
717 EMBO J. 2007 Apr 18;26(8):2127–36.
718 56. Gowrishankar R, Gresch PJ, Davis GL, Katamish RM, Riele JR, Stewart AM, et al. Region-
719 Specific Regulation of Presynaptic Dopamine Homeostasis by D2 Autoreceptors Shapes
720 the In Vivo Impact of the Neuropsychiatric Disease-Associated DAT Variant Val559. J
721 Neurosci. 2018 Jun 6;38(23):5302–12.
722 57. Luethi D, Liechti ME. Designer drugs: mechanism of action and adverse effects. Arch
723 Toxicol. 2020 Apr;94(4):1085–133.
724 58. Svingos AL, Chavkin C, Colago EE, Pickel VM. Major coexpression of kappa-opioid
725 receptors and the dopamine transporter in nucleus accumbens axonal profiles. Synapse.
726 2001 Dec 1;42(3):185–92.
727 59. Margolis EB, Hjelmstad GO, Bonci A, Fields HL. Kappa-opioid agonists directly inhibit
728 midbrain dopaminergic neurons. J Neurosci. 2003 Nov 5;23(31):9981–6.

60. Land BB, Bruchas MR, Lemos JC, Xu M, Melief EJ, Chavkin C. The dysphoric component of stress is encoded by activation of the dynorphin kappa-opioid system. J Neurosci. 2008 Jan 9;28(2):407–14.
61. Kozono H, Yoshitani H, Nakano R. Post-marketing surveillance study of the safety and efficacy of nalfurafine hydrochloride (Remitch® capsules 2.5 µg) in 3,762 hemodialysis patients with intractable pruritus. Int J Nephrol Renovasc Dis. 2018;11:9–24.
62. Reed B, Butelman ER, Fry RS, Kimani R, Kreek MJ. Repeated Administration of Opra Kappa (LY2456302), a Novel, Short-Acting, Selective KOP-r Antagonist, in Persons with and without Cocaine Dependence. Neuropsychopharmacology. 2018 Mar;43(4):928.
63. Lowe SL, Wong CJ, Witcher J, Gonzales CR, Dickinson GL, Bell RL, et al. Safety, tolerability, and pharmacokinetic evaluation of single- and multiple-ascending doses of a novel kappa opioid receptor antagonist LY2456302 and drug interaction with ethanol in healthy subjects. J Clin Pharmacol. 2014 Sep;54(9):968–78.
64. Krystal AD, Pizzagalli DA, Smoski M, Mathew SJ, Nurnberger J, Lisanby SH, et al. A randomized proof-of-mechanism trial applying the “fast-fail” approach to evaluating κ-opioid antagonism as a treatment for anhedonia. Nat Med. 2020 May;26(5):760–8.
65. Pizzagalli DA, Smoski M, Ang YS, Whitton AE, Sanacora G, Mathew SJ, et al. Selective kappa-opioid antagonism ameliorates anhedonic behavior: evidence from the Fast-fail Trial in Mood and Anxiety Spectrum Disorders (FAST-MAS). Neuropsychopharmacology. 2020 Sep;45(10):1656–63.
66. Foster JD, Yang JW, Moritz AE, Challasivakanaka S, Smith MA, Holy M, et al. Dopamine transporter phosphorylation site threonine 53 regulates substrate reuptake and amphetamine-stimulated efflux. J Biol Chem. 2012 Aug 24;287(35):29702–12.
67. Mowlem FD, Rosenqvist MA, Martin J, Lichtenstein P, Asherson P, Larsson H. Sex differences in predicting ADHD clinical diagnosis and pharmacological treatment. Eur Child Adolesc Psychiatry. 2019 Apr;28(4):481–9.
68. Daws LC, Owens WA, Toney GM. Using High-Speed Chronoamperometry to Measure Biogenic Amine Release and Uptake In Vivo. In 2016. p. 53–81.
69. Mayer FP, Niello M, Cintulova D, Sideromenos S, Maier J, Li Y, et al. Serotonin-releasing agents with reduced off-target effects. Mol Psychiatry. 2023 Feb;28(2):722–32.
70. Ramamoorthy S, Shippenberg TS, Jayanthi LD. Regulation of monoamine transporters: Role of transporter phosphorylation. Pharmacol Ther. 2011 Feb;129(2):220–38.
71. Foster JD, Vaughan RA. Phosphorylation mechanisms in dopamine transporter regulation. J Chem Neuroanat. 2017 Oct;83–84:10–8.
72. Gorentla BK, Moritz AE, Foster JD, Vaughan RA. Proline-directed phosphorylation of the dopamine transporter N-terminal domain. Biochemistry. 2009 Feb 10;48(5):1067–76.
73. Challasivakanaka S, Zhen J, Smith ME, Reith MEA, Foster JD, Vaughan RA. Dopamine transporter phosphorylation site threonine 53 is stimulated by amphetamines and regulates dopamine transport, efflux, and cocaine analog binding. J Biol Chem. 2017 Nov 17;292(46):19066–75.
74. Ragu Varman D, Subler MA, Windle JJ, Jayanthi LD, Ramamoorthy S. Novelty-induced hyperactivity and suppressed cocaine induced locomotor activation in mice lacking threonine 53 phosphorylation of dopamine transporter. Behavioural brain research. 2021 Jun 25;408:113267.

773 75. Li LB, Chen N, Ramamoorthy S, Chi L, Cui XN, Wang LC, et al. The role of N-glycosylation
774 in function and surface trafficking of the human dopamine transporter. J Biol Chem. 2004
775 May 14;279(20):21012–20.
776 76. Gulley JM, Larson GA, Zahniser NR. Using High-Speed Chronoamperometry with Local
777 Dopamine Application to Assess Dopamine Transporter Function. 2007.
778 77. Horan P, Taylor J, Yamamura HI, Porreca F. Extremely long-lasting antagonistic actions of
779 nor-binaltorphimine (nor-BNI) in the mouse tail-flick test. J Pharmacol Exp Ther. 1992
780 Mar;260(3):1237–43.
781 78. Bruchas MR, Yang T, Schreiber S, Defino M, Kwan SC, Li S, et al. Long-acting kappa opioid
782 antagonists disrupt receptor signaling and produce noncompetitive effects by activating
783 c-Jun N-terminal kinase. J Biol Chem. 2007 Oct 12;282(41):29803–11.
784 79. Prut L, Belzung C. The open field as a paradigm to measure the effects of drugs on
785 anxiety-like behaviors: a review. Eur J Pharmacol. 2003 Feb 28;463(1–3):3–33.
786 80. Volkow ND, Wang GJ, Newcorn J, Fowler JS, Telang F, Solanto M V, et al. Brain dopamine
787 transporter levels in treatment and drug naïve adults with ADHD. Neuroimage. 2007 Feb
788 1;34(3):1182–90.
789 81. Howes OD, McCutcheon R, Owen MJ, Murray RM. The Role of Genes, Stress, and
790 Dopamine in the Development of Schizophrenia. Biol Psychiatry. 2017 Jan 1;81(1):9–20.
791 82. Jeste SS, Geschwind DH. Disentangling the heterogeneity of autism spectrum disorder
792 through genetic findings. Nat Rev Neurol. 2014 Feb;10(2):74–81.
793 83. Wang YM, Gainetdinov RR, Fumagalli F, Xu F, Jones SR, Bock CB, et al. Knockout of the
794 vesicular monoamine transporter 2 gene results in neonatal death and supersensitivity to
795 cocaine and amphetamine. Neuron. 1997 Dec;19(6):1285–96.
796 84. Zhou QY, Palmiter RD. Dopamine-deficient mice are severely hypoactive, adipsic, and
797 aphagic. Cell. 1995 Dec 29;83(7):1197–209.
798 85. Kurian MA, Zhen J, Cheng SY, Li Y, Mordekar SR, Jardine P, et al. Homozygous loss-of-
799 function mutations in the gene encoding the dopamine transporter are associated with
800 infantile parkinsonism-dystonia. J Clin Invest. 2009 Jun;119(6):1595–603.
801 86. Kurian MA. SLC6A3-Related Dopamine Transporter Deficiency Syndrome. 1993.
802 87. Mayer FP, Stewart A, Blakely RD. Leaky lessons learned: Efflux prone dopamine
803 transporter variant reveals sex and circuit specific contributions of D2 receptor signalling
804 to neuropsychiatric disease. Basic Clin Pharmacol Toxicol. 2024 Feb;134(2):206–18.
805 88. Azocar VH, Sepúlveda G, Ruiz C, Aguilera C, Andrés ME, Fuentealba JA. The blocking of
806 kappa-opioid receptor reverses the changes in dorsolateral striatum dopamine dynamics
807 during the amphetamine sensitization. J Neurochem. 2019 Feb;148(3):348–58.
808 89. Thompson AC, Zapata A, Justice JB, Vaughan RA, Sharpe LG, Shippenberg TS. Kappa-
809 opioid receptor activation modifies dopamine uptake in the nucleus accumbens and
810 opposes the effects of cocaine. J Neurosci. 2000 Dec 15;20(24):9333–40.
811 90. Van’t Veer A, Bechtholt AJ, Onvani S, Potter D, Wang Y, Liu-Chen LY, et al. Ablation of
812 kappa-opioid receptors from brain dopamine neurons has anxiolytic-like effects and
813 enhances cocaine-induced plasticity. Neuropsychopharmacology. 2013 Jul;38(8):1585–
814 97.

815 91. Pomrenze MB, Cardozo Pinto DF, Neumann PA, Llorach P, Tucciarone JM, Morishita W, et
816 al. Modulation of 5-HT release by dynorphin mediates social deficits during opioid
817 withdrawal. Neuron. 2022 Dec 21;110(24):4125-4143.e6.
818 92. Lycas MD, Ejdrup AL, Sørensen AT, Haahr NO, Jørgensen SH, Guthrie DA, et al.
819 Nanoscopic dopamine transporter distribution and conformation are inversely regulated
820 by excitatory drive and D2 autoreceptor activity. Cell Rep. 2022 Sep 27;40(13):111431.
821 93. Belovich AN, Aguilar JI, Mabry SJ, Cheng MH, Zanella D, Hamilton PJ, et al. A network of
822 phosphatidylinositol (4,5)-bisphosphate (PIP2) binding sites on the dopamine transporter
823 regulates amphetamine behavior in Drosophila Melanogaster. Mol Psychiatry. 2021
824 Aug;26(8):4417–30.
825 94. Hamilton PJ, Belovich AN, Khelashvili G, Saunders C, Erreger K, Javitch JA, et al. PIP2
826 regulates psychostimulant behaviors through its interaction with a membrane protein.
827 Nat Chem Biol. 2014 Jul;10(7):582–9.
828 95. Binda F, Dipace C, Bowton E, Robertson SD, Lute BJ, Fog JU, et al. Syntaxin 1A interaction
829 with the dopamine transporter promotes amphetamine-induced dopamine efflux. Mol
830 Pharmacol. 2008 Oct;74(4):1101–8.
831 96. Buchmayer F, Schicker K, Steinkellner T, Geier P, Stübiger G, Hamilton PJ, et al.
832 Amphetamine actions at the serotonin transporter rely on the availability of
833 phosphatidylinositol-4,5-bisphosphate. Proc Natl Acad Sci U S A. 2013 Jul
834 9;110(28):11642–7.
835 97. Lalonde R. The neurobiological basis of spontaneous alternation. Neurosci Biobehav Rev.
836 2002 Jan;26(1):91–104.
837 98. Zhang L, McCarthy DM, Eskow Jaunarajs KL, Biederman J, Spencer TJ, Bhide PG. Frontal
838 Cortical Monoamine Release, Attention, and Working Memory in a Perinatal Nicotine
839 Exposure Mouse Model Following Kappa Opioid Receptor Antagonism. Cereb Cortex.
840 2021 Jan 1;31(1):483–96.
841 99. Dwyer JB, Cardenas A, Franke RM, Chen Y, Bai Y, Belluzzi JD, et al. Prenatal nicotine sex-
842 dependently alters adolescent dopamine system development. Transl Psychiatry. 2019
843 Nov 18;9(1):304.
844 100. Zhou FM, Liang Y, Dani JA. Endogenous nicotinic cholinergic activity regulates dopamine
845 release in the striatum. Nat Neurosci. 2001 Dec;4(12):1224–9.
846

847

848 **Figure 1**

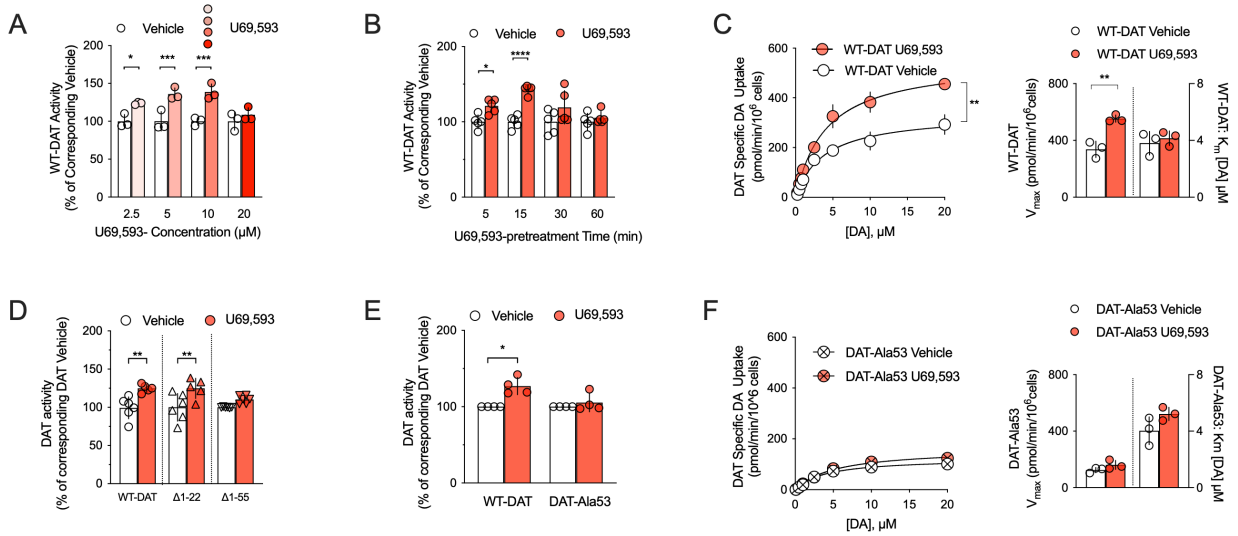

849

850 **Figure 1: The KOR agonist U69,593 increases DAT-mediated uptake via a Thr53 dependent mechanism.**
851 EM4 cells were transfected with DAT and KOR and uptake of [^{3}H]DA was assessed as described in
852 Methods.
853 **A**: U69,593 (10 μM) increased WT DAT-mediated uptake in rDAT/rKOR cotransfected EM4 cells in a
854 concentration-dependent manner as compared to vehicle (n= 3 independent observations per
855 condition, one-way ANOVA, followed by Bonferroni post-hoc tests).
856 **B**: Treatment with 10 μM U69,593 enhanced WT DAT specific uptake in a time-dependent fashion (n= 5
857 independent observations per condition, one-way ANOVA, followed by Bonferroni post-hoc tests).
858 **C**: Incubation with 10 μM U69,593 increased WT DAT V_{max} (two-tailed unpaired t-test) without effect on
859 K_M (n=3 independent observations per condition, two-tailed Student's unpaired t-test).
860 **D**: Treatment with U69,593 significantly augmented WT DAT-mediated uptake when compared to
861 vehicle in cells that expressed KOR plus either WT DAT or a truncated version of DAT, lacking the first 22
862 N-terminal residues (DAT Δ1-22). In contrast, truncation of the first 55 N-terminal residues (DAT Δ1-55
863 DAT) prevented KOR-agonist induced increases in [^{3}H]DA uptake. (n=5-6 independent observations per
864 condition, one-way ANOVA, followed by Bonferroni post-hoc tests)
865 **E**: Site-directed mutagenesis of DAT Thr53 to alanine (DAT-Ala53) rendered transporter-mediated DA
866 uptake insensitive to pre-treatment with U69,593 at 5 and 10 μM (n=4 observations per condition, One-
867 way ANOVA, followed by Bonferroni posthoc tests).
868 **F**: U69,593 did not affect the kinetic parameters K_M and V_{max} of the DAT-Ala53 mutant (n=3 independent
869 observations per condition, Student's two-tailed unpaired t-test)
870 Data are shown as the mean with error bars reflecting the SD *=P<0.05; **=P<0.01; ***=P<0.001;
871 ****=P<0.0001.

872 **Figure 2**

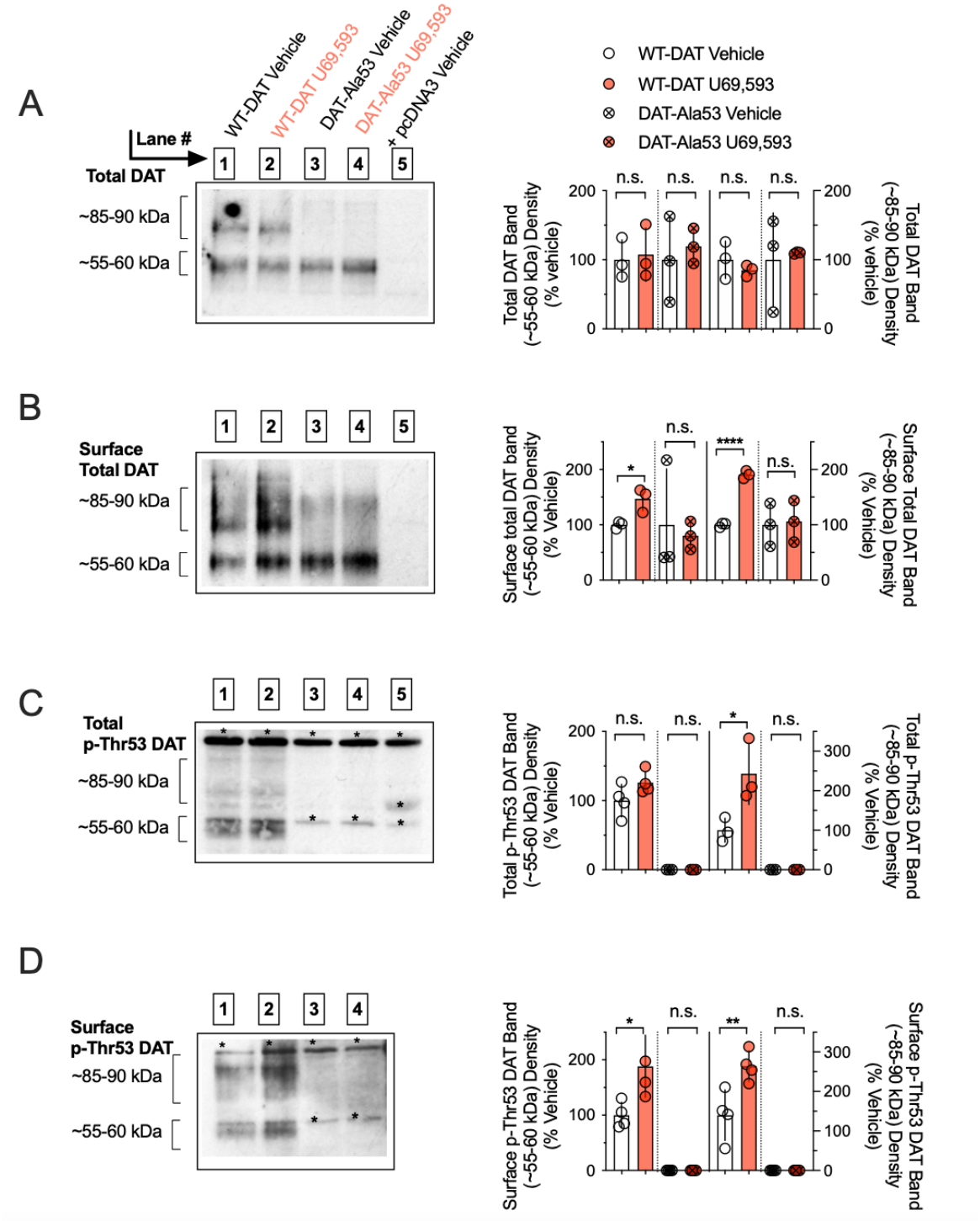

873

874 **Figure 2: Capacity to phosphorylate rDAT at Thr53 is required for rKOR activation to elevate**
875 **transporter surface expression**
876 EM4 cells were transfected with either WT DAT or DAT Ala53 plus rKOR, subjected to U69,593 and
877 biotinylated as described in Methods.

878 **A**: Treatment with U69,593 did not affect WT DAT band densities at ~55-60 kDa and ~85-90 kDa, derived
879 from total protein lysates (n=3 independent observations per condition, Student's two-tailed unpaired t-
880 test).
881 **B**: Incubation with U69,593 increased the WT DAT band densities at ~55-60 kDa and ~85-90 kDa, derived
882 from biotinylated protein lysates (unpaired, two-tailed t-test). No effect was observed on the DAT Ala53
883 band densities at ~55-60 kDa (n=3 independent observations per condition, Student's two-tailed
884 unpaired t-test).
885 C and D: Protein lysates were immunoblotted with p-Thr53 antibody. Bands marked with an asterisk
886 indicate non-specific immunoreactivity.
887 **C**: In total protein lysates, incubation with U69,593 increased the density of the p-Thr53 immunoreactive
888 band at ~55-60 kDa for WT DAT (Student's unpaired, two-tailed t-test). No effect was observed on the
889 band densities at ~85-90 kDa. No specific bands were detected for the DAT Ala53 variant (n=3-5
890 independent observations per condition, Student's two-tailed unpaired t-test).
891 **D**: U69,593 augmented band densities at ~55-60 and ~85-90 kDa for biotinylated WT DAT (n=5
892 independent observations per condition, Student's two-tailed unpaired t-test). No specific bands were
893 detected for the DAT Ala53 variant.
894 All bars represent the mean with error bars reflecting the SD. Individual quantifications are displayed as
895 individual symbols. *=P<0.05; **=P<0.01; ****=P<0.0001. n.s.=not significant
896

897 **Figure 3**

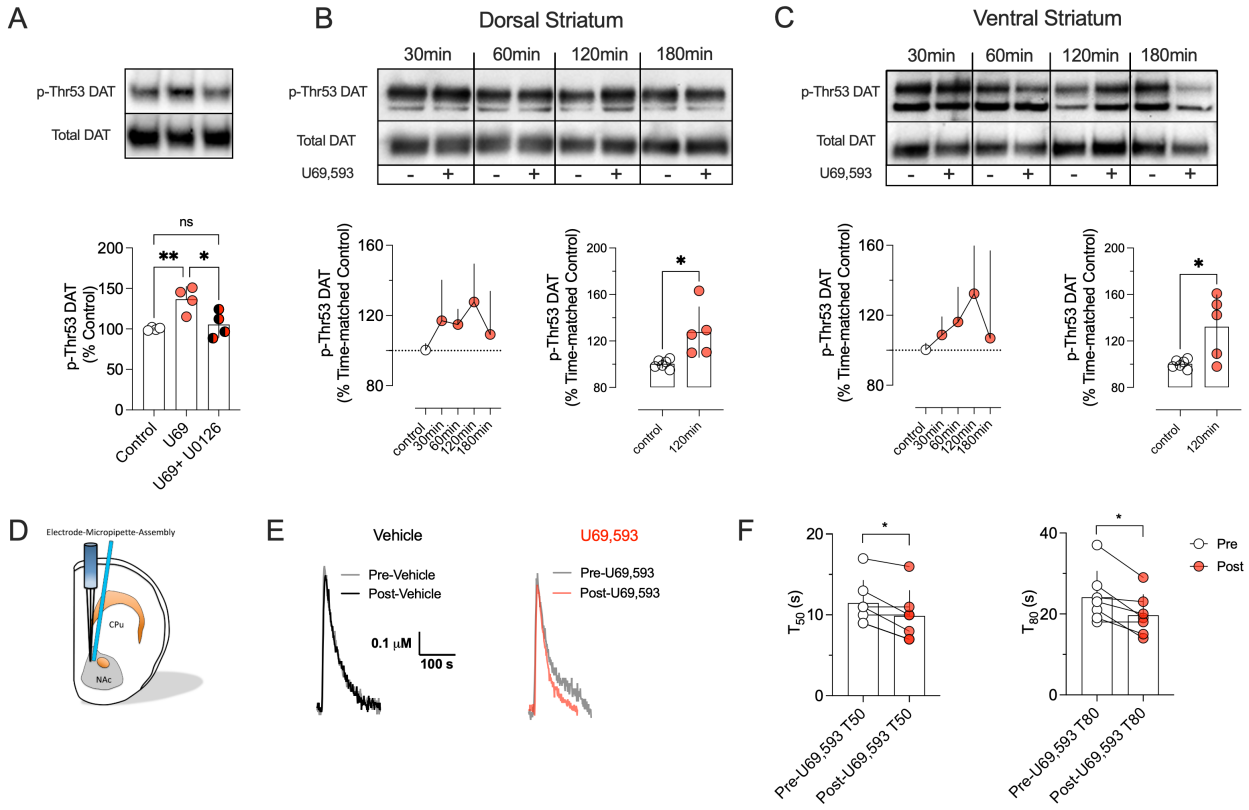

898

899 **Figure 3: KOR-agonism enhances phosphorylation of DAT at Thr53 in native preparations and**
900 **augments DAT-mediated clearance in the NAc *in vivo*.**
901 **A)** Male rat striatal synaptosomes were treated with vehicle or 50 µM U0126 for 15 min at 30˚C,
902 followed by treatment with vehicle or 10 µM U69,593 for an additional 15 min 30˚C. After treatment,
903 samples were subjected to SDS-PAGE and western blotted for total and p-Thr53 DAT. Upper panel
904 shows representative western blots. Lower panel shows quantification of p-Thr53 DAT staining as a
905 percentage of basal levels. (n=4; one-way ANOVA, Tukey's multiple comparisons test).
906 **B and C)** Rats were injected s.c. with vehicle or U69,593 (0.32 mg/kg) and sacrificed at indicated times.
907 Tissue from the dorsal **(B)** or ventral striatum **(C)** were western blotted for total and p-Thr53 DAT in
908 duplicate. Signals from the U69,593 treated samples were compared to the time-matched control. The
909 upper panels show representative western blots for the dorsal and ventral striatum with each time-
910 matched control followed by U69,593 treatment. The lower panels show quantification of the p-Thr53
911 DAT staining as a percentage of the time-matched control (Two-tailed, unpaired t-test).
912 **D**) Schematic representation of the electrode-micropipette assembly that was lowered into the NAc of
913 anaesthetized rats to allow for *in vivo* chromatographic measurement of DA clearance rates.
914 **E**) Representative oxidation currents converted to micromolar values observed upon pressure ejection
915 of DA before (gray traces) and 2 min after intra-NAc injection of vehicle (black trace), U69,593 (890 µM,
916 barrel concentration, red trace). The leftward-shift in the representative trace following U69,593
917 injection is indicative of increased DA clearance.
918 **F**) U69,593 decreased the clearance time of exogenously applied DA in the NAc (T_{50} and T_{80}; n= 7
919 observations per condition, two-tailed paired t-test) when compared to the pre-drug value. Bars indicate
920 the mean and error reflect SD. Individual values from each animal are reflected by the corresponding
921 symbols. *denotes P<0.05; **denotes P<0.01, ns = not significant.

Figure 4

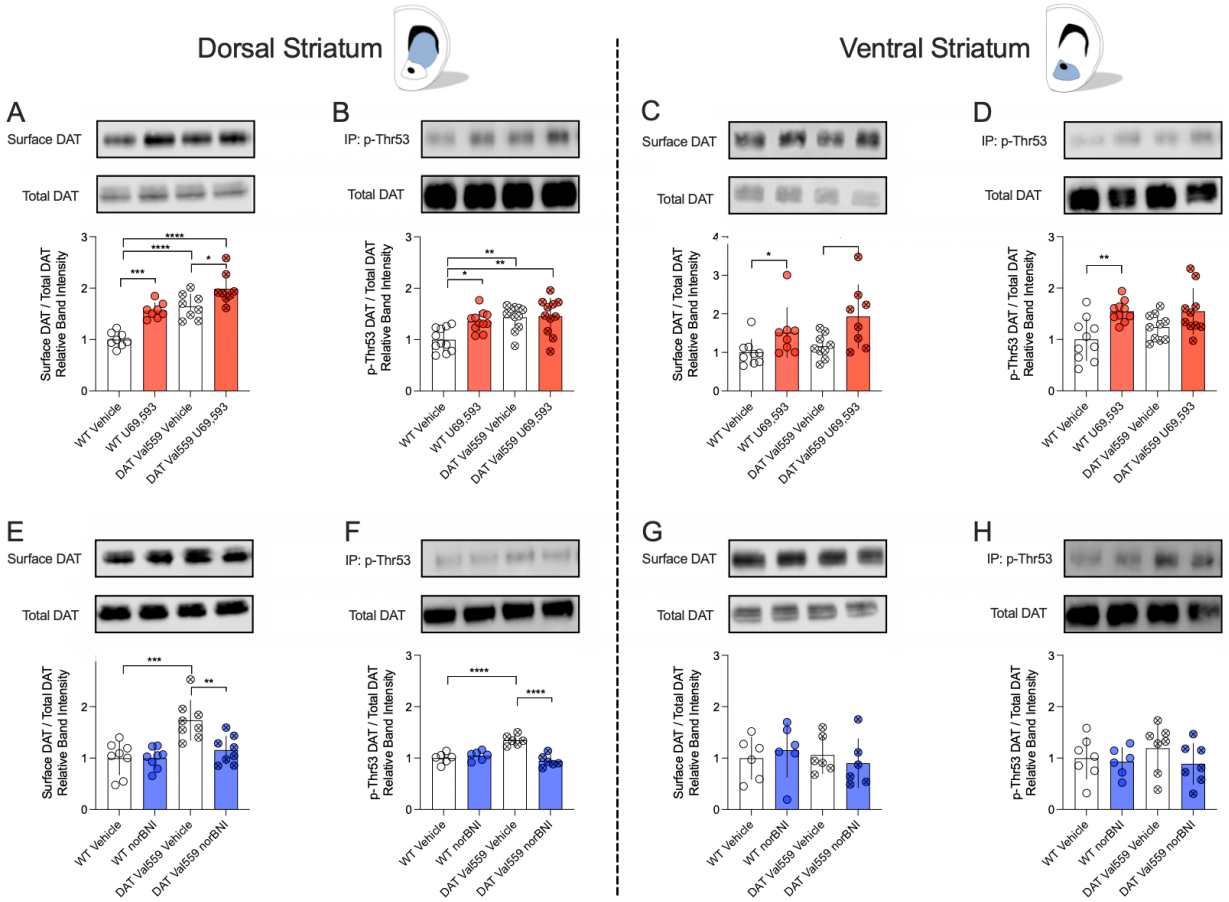

Figure 4: mKOR agonism induces enhanced mDAT surface expression and phosphorylation at mDAT Thr53 while mKOR antagonism normalizes enhanced surface expression and Thr53 phosphorylation of mDAT Val559 in acute brain slices containing the DS or VS

A-D) Acute slices containing the DS and/or the VS were exposed to 10 µM of U69,693 or vehicle for 7 min and surface expression and phosphorylation of p-Thr53 DAT was assessed.

A and **B)** In the DS, treatment with U69,593 increased surface DAT levels (A) (n=9; two-way ANOVA, Šídák's multiple comparisons test) as well as phosphorylation of mDAT at Thr53 (B) (n=10; two-way ANOVA, Šídák's multiple comparisons test). Higher basal phosphorylation levels at Thr53 were detected for the DAT Val559 when compared to WT DAT in the DS (n=11; two-way ANOVA, Šídák's multiple comparisons test).

C) In the VS, KOR-agonist treatment increased surface mDAT levels independent of genotype as compared to vehicle treatment (n=8; two-way ANOVA, Šídák's multiple comparisons test).

D) Treatment with U69,593 enhanced WT mDAT phosphorylation at Thr53, but remained without effect on DAT Val559 phosphorylation.

E-H) Acute coronal slices containing the DS or the VS were treated with the KOR antagonist norBNI (1 µM) for 20 min and DAT surface expression and phosphorylation at Thr53 were determined.

E and **F)** In the DS, antagonism of mKOR reduced the enhanced surface expression **(E)** (n=8; two-way ANOVA, Šídák's multiple comparisons test) and Thr-53 phosphorylation **(F)** (n=6; two-way ANOVA, Šídák's multiple comparisons test) of tansporters in DAT Val559 mice. No effect of norBNI was detected on WT DAT.

944 **G** and **H)** Treatment with norBNI remained without effect on DAT surface expression **(G)** (n=6, two-way
945 ANOVA, Šídák's multiple comparisons test) and Thr-53 phosphorylation **(H)** (n= 7, two-way ANOVA,
946 Šídák's multiple comparisons test) in the VS.
947 All bars show the mean and SD. Symbols reflect individual observations. * = $P \leq 0.05$, ** = $P \leq 0.01$, *** =
948 $P \leq 0.001$, **** = $P \leq 0.0001$

Figure 5

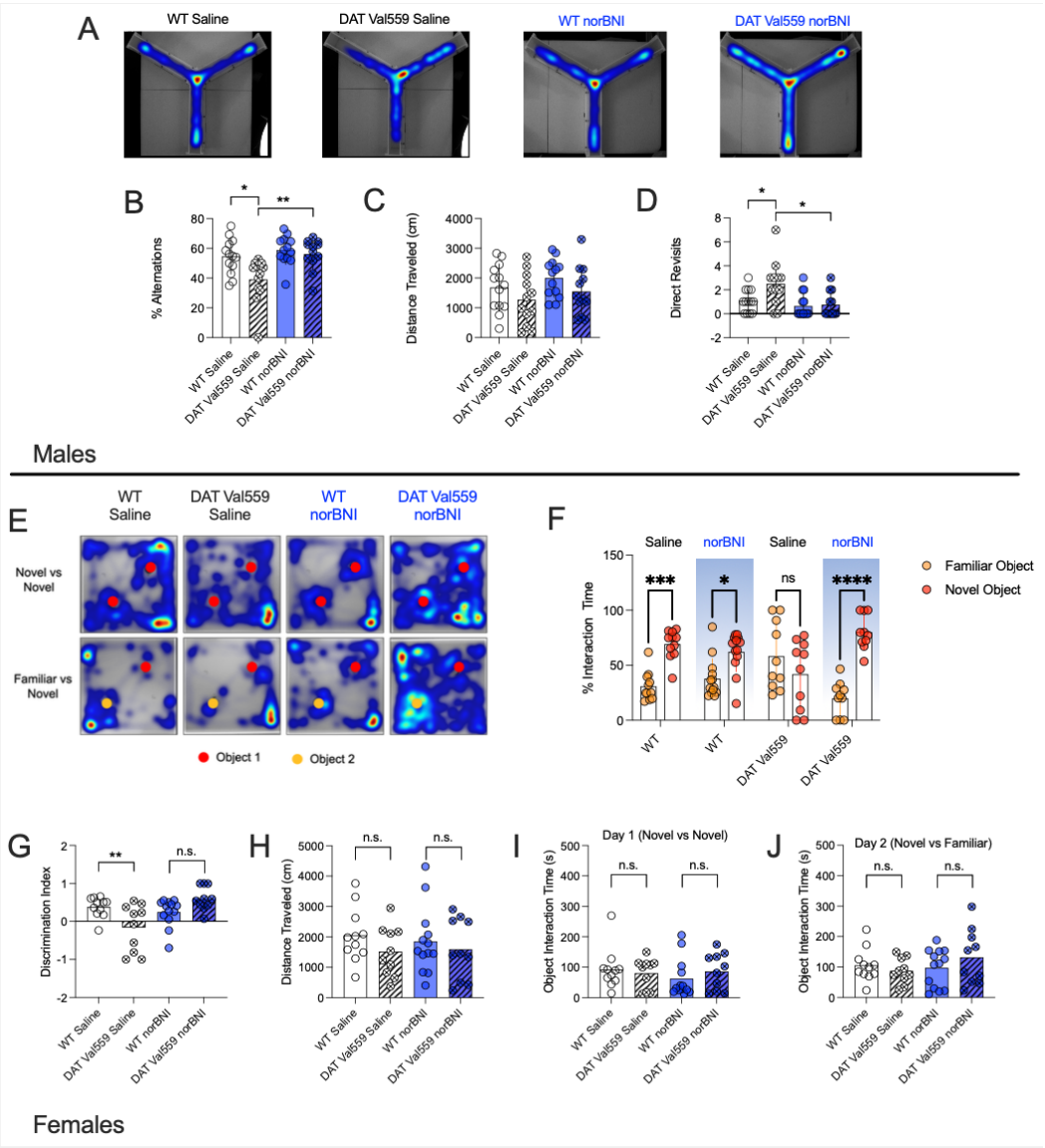

Figure 5: Treatment with norBNI normalizes sex-specific behavioral phenotypes of male and female DAT Val559 mice

A-D) Male homozygous DAT Val559 mice and their WT littermates were injected with saline (vehicle; n= 13 for WT and 12 for DAT Val559, respectively) or norBNI (10 mg / kg, i.p.; n= 13 for WT and 12 for DAT Val559, respectively) 30 min prior to testing, placed into the center of the open Y-maze and the number of alternating arm entries, distance travelled and direct revisits were recorded as described in Methods.
A) Representative heat maps showing the explorative behavior of WT and Val559 mice following vehicle or norBNI administration. Time spent in each area is directly correlated to the color gradient ranging from dark blue to dark red, with the latter indicating highest value.
B) Systemic administration of norBNI 30 min prior to the test normalized the deficit in the percentage of alternations of DAT Val559 mice when compared to WT control mice.
C) No acute effect of norBNI was observed for total distance travelled during the test session.
D) Administration of norBNI reduced the number of direct revisits of DAT Val559 mice.

964 E-J) The NOR task was performed with saline treated female WT (n=11) and DAT Val559 littermates
965 (n=10) and compared to norBNI treated (10 mg/kg, i.p., 30 min prior to testing) female WT (n=13) and
966 littermate DAT Val559 (n=10) mice.
967 E) provides representative heat maps representing location in relation to objects (circles) used in NOR
968 sessions. The relative interaction time with the familiar versus the novel object and the discrimination
969 index are shown in (F) and (G), respectively.
970 H) shows the total distance travelled and the total object interaction times on day 1 (two novel objects)
971 and day 2 (one novel and one familiar object) are shown in panels (I) and (J), respectively.
972 Data are given as mean and SD and were analyzed using two-way ANOVA with Šídák's multiple
973 comparisons test. *=P<0.05, **=P<0.01, ***=P<0.001, ****=P<0.0001, n.s.= not significant.

974 **Figure 6**

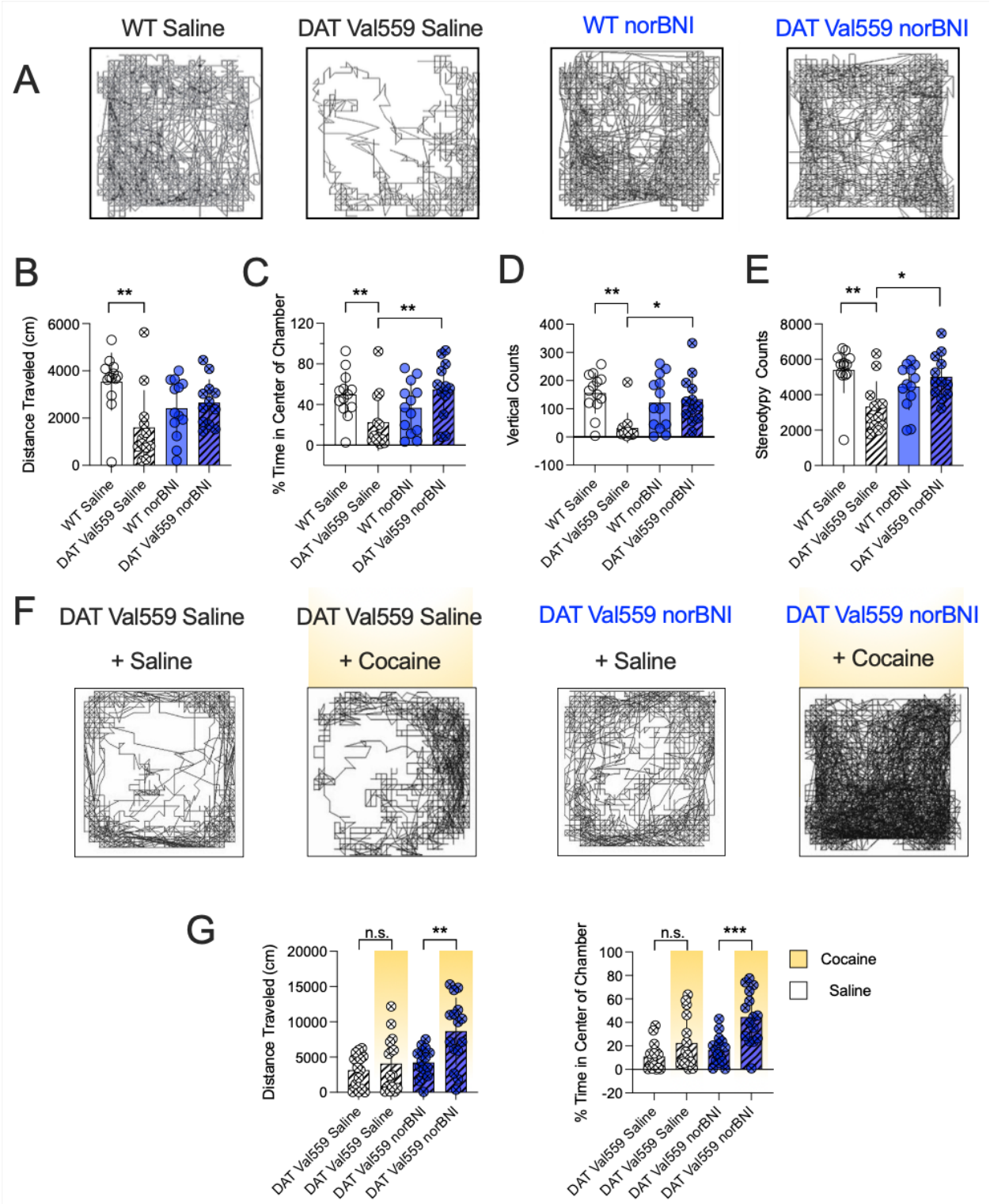

975
976 **Figure 6 norBNI treatment of male DAT Val559 mice normalizes abnormal locomotor responses to**
977 **injection stress and locomotor response to systemic cocaine as monitored in the open field test**
978 A-E) Homozygous male DAT Val559 and WT littermates were injected with saline (vehicle) or norBNI (10
979 mg/kg, i.p.) and placed in open activity chambers one week post injection.

A) Representative activity traces of WT and DAT Val559 mice. DAT Val559 mice previously injected with vehicle (saline) displayed significantly less B) forward locomotor activity C) spent less time in the center of the activity chamber and exhibited fewer
D) vertical counts and E) stereotypies when compared to WT mice. No differences between genotypes were detected when the mice were pretreated with norBNI.
F-G) Homozygous male DAT Val559 were injected with saline or cocaine (10 mg/kg, i.p.) one week post administration of norBNI (10 mg/kg, i.p.) and placed into open activity chambers.
F) Representative traces of male DAT Val559 mice injected with the indicated drug combinations. G) Total distance travelled and time spent in the center of the chamber of male DAT Val559 mice injected with the indicated combinations of saline, norBNI and cocaine.
All bars show the mean and SD. n=12-13 individual animals per group, data in B, C, D, E and G were analyzed with two-way ANOVA, Šídák's multiple comparisons test. Symbols reflect individual animals. * = $P \leq 0.05$, ** = $P \leq 0.01$, *** = $P \leq 0.001$, ns = not significant.

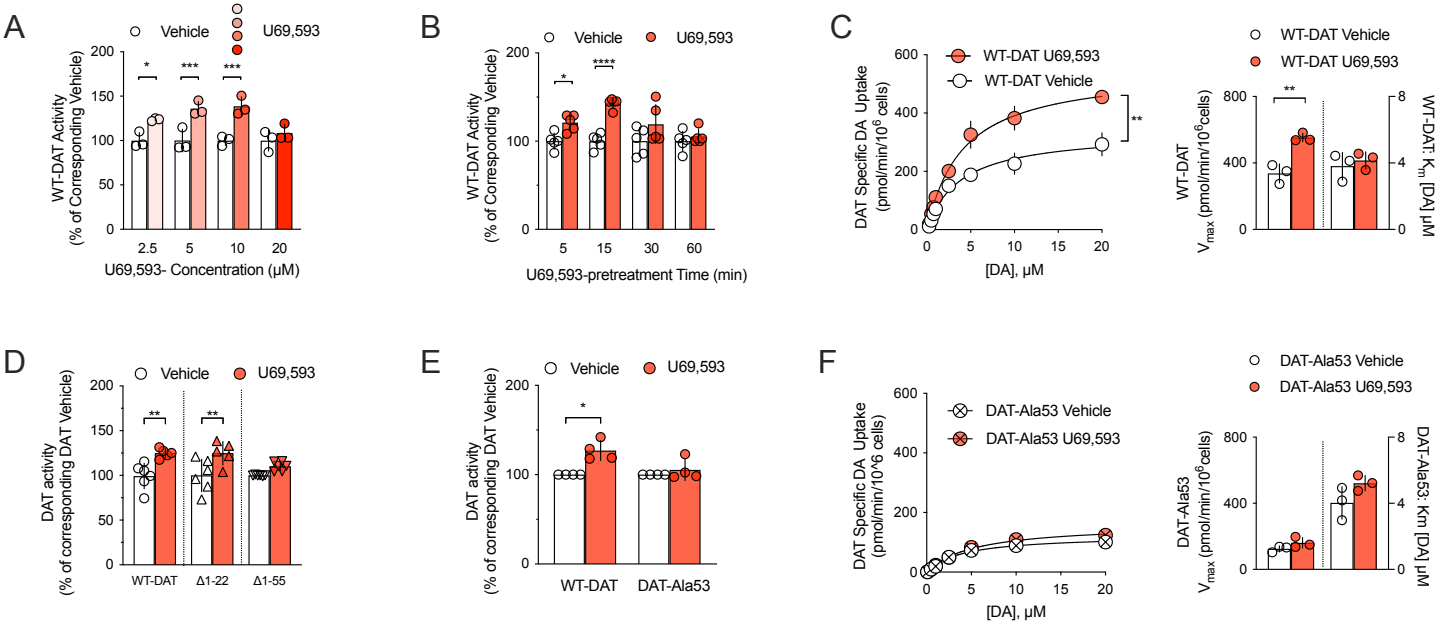
A
Vehicle
U69,593
WT-DAT Activity
(% of Corresponding Vehicle)
U69,593- Concentration (μM)
B
Vehicle
U69,593
WT-DAT Activity
(% of Corresponding Vehicle)
U69,593-pretreatment Time (min)
C
WT-DAT U69,593
WT-DAT Vehicle
DAT Specific DA Uptake
(pmol/min/10^6 cells)
[DA], μM
WT-DAT Vehicle
WT-DAT U69,593
WT-DAT
Vmax (pmol/min/10^6cells)
WT-DAT: Km [DA] μM
D
Vehicle
U69,593
DAT activity
(% of corresponding DAT Vehicle)
WT-DAT
Δ1-22
Δ1-55
E
Vehicle
U69,593
DAT activity
(% of corresponding DAT Vehicle)
WT-DAT
DAT-Ala53
F
DAT-Ala53 Vehicle
DAT-Ala53 U69,593
DAT Specific DA Uptake
(pmol/min/10^6 cells)
[DA], μM
DAT-Ala53 Vehicle
DAT-Ala53 U69,593
DAT-Ala53
Vmax (pmol/min/10^6cells)
DAT-Ala53: Km [DA] μM

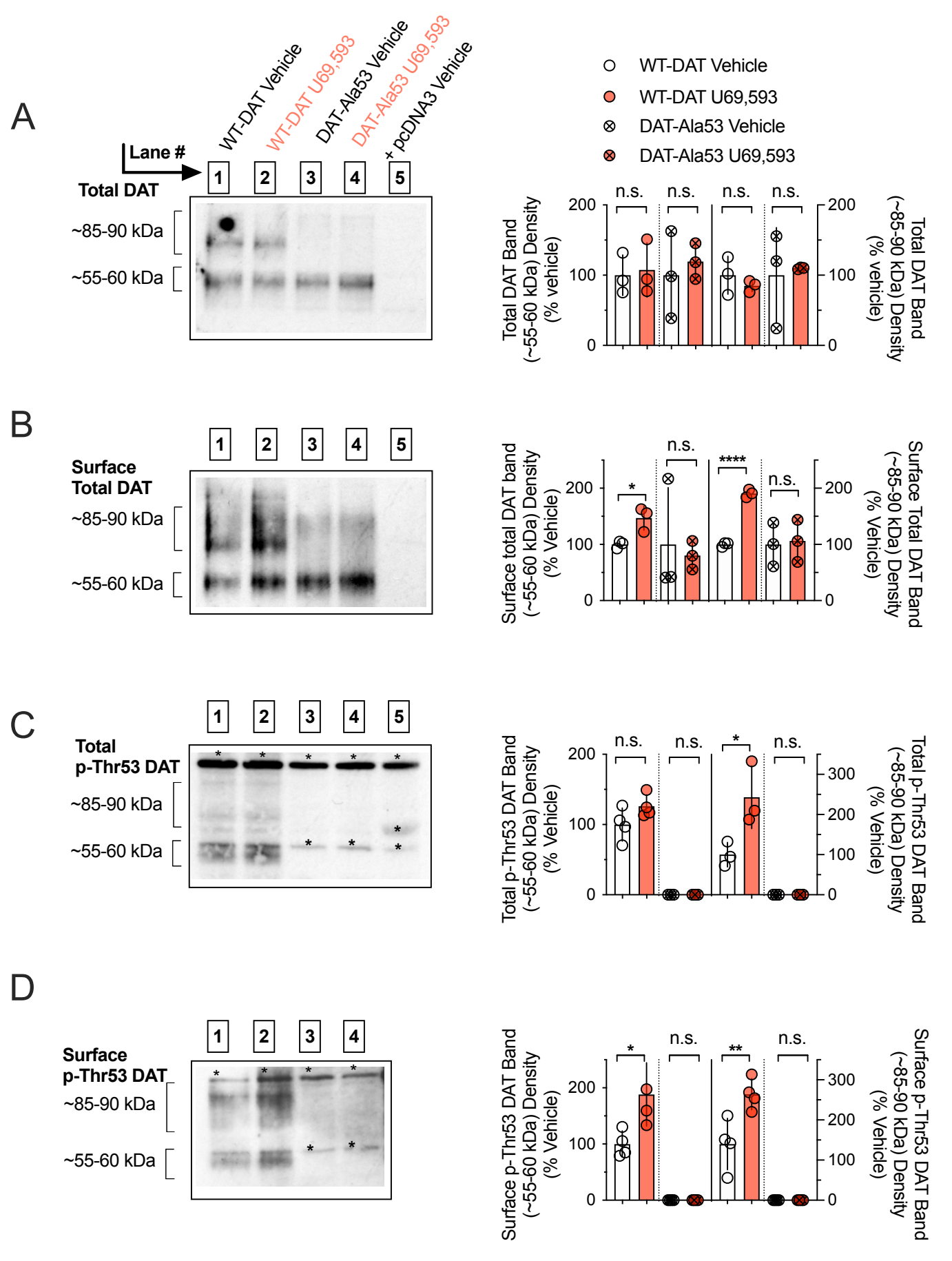
A
WT-DAT Vehicle
WT-DAT U69,593
DAT-Ala53 Vehicle
DAT-Ala53 U69,593
+ pcDNA3 Vehicle
Lane #
1
2
3
4
5
Total DAT
~85-90 kDa
~55-60 kDa
Total DAT Band (~55-60 kDa) Density (% vehicle)
Total DAT Band (~85-90 kDa) Density (% vehicle)
n.s.
B
Surface Total DAT
Surface total DAT band (~55-60 kDa) Density (% Vehicle)
Surface Total DAT Band (~85-90 kDa) Density (% Vehicle)
*
****
C
Total p-Thr53 DAT
Total p-Thr53 DAT Band (~55-60 kDa) Density (% Vehicle)
Total p-Thr53 DAT Band (~85-90 kDa) Density (% Vehicle)
D
Surface p-Thr53 DAT
Surface p-Thr53 DAT Band (~55-60 kDa) Density (% Vehicle)
Surface p-Thr53 DAT Band (~85-90 kDa) Density (% Vehicle)
**

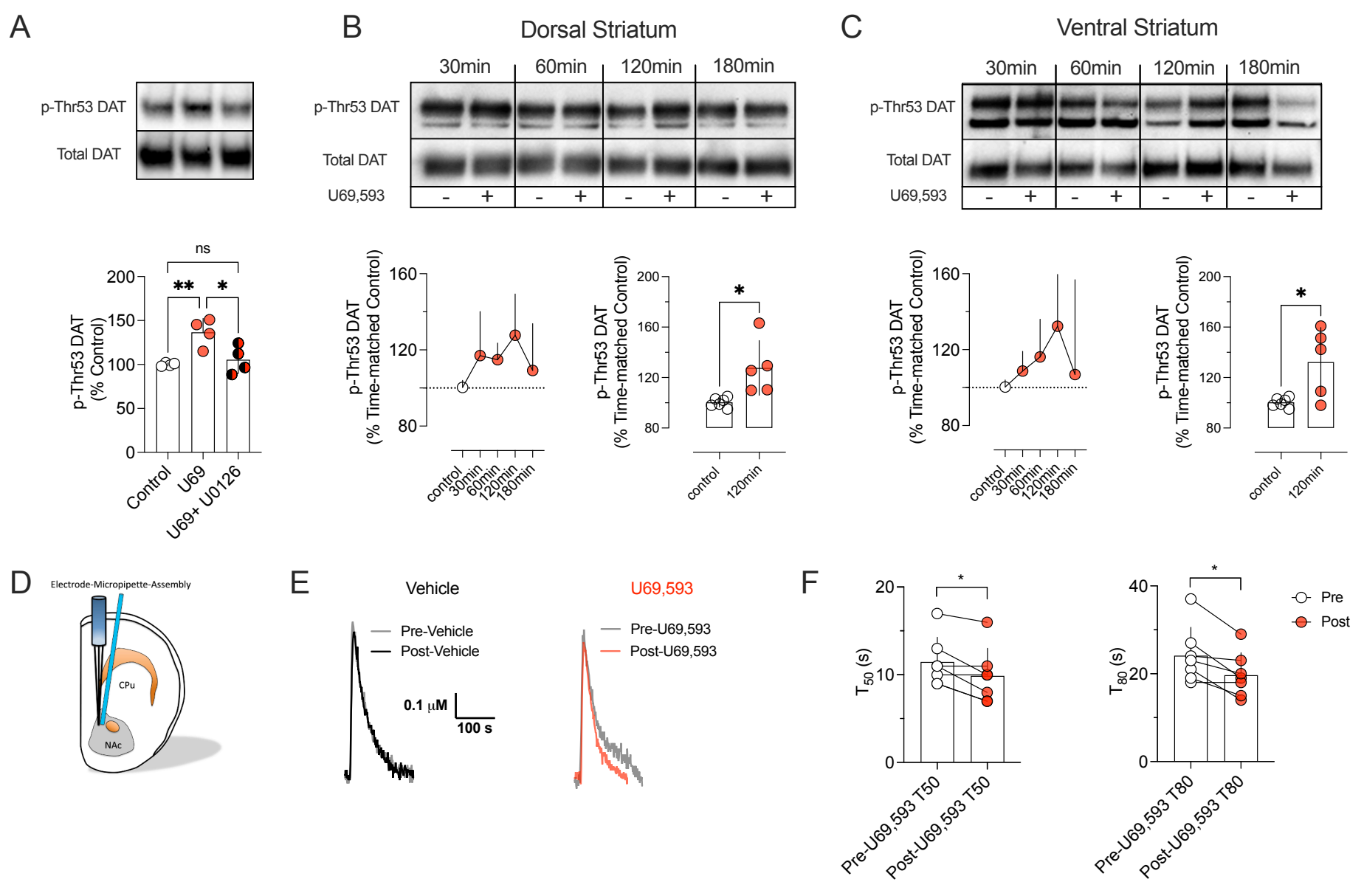
A
p-Thr53 DAT
Total DAT
ns
**
*
p-Thr53 DAT (% Control)
200
150
100
50
0
Control
U69
U69+ U0126
B
Dorsal Striatum
30min
60min
120min
180min
p-Thr53 DAT
Total DAT
U69,593
- + - + - + - +
p-Thr53 DAT (% Time-matched Control)
160
120
80
control
30min
60min
120min
180min
*
200
160
120
80
control
120min
C
Ventral Striatum
30min
60min
120min
180min
p-Thr53 DAT
Total DAT
U69,593
- + - + - + - +
p-Thr53 DAT (% Time-matched Control)
160
120
80
control
30min
60min
120min
180min
*
200
160
120
80
control
120min
D
Electrode-Micropipette-Assembly
CPu
NAc
E
Vehicle
Pre-Vehicle
Post-Vehicle
0.1 μM
100 s
U69,593
Pre-U69,593
Post-U69,593
F
*
20
10
0
T50 (s)
Pre-U69,593 T50
Post-U69,593 T50
*
40
20
0
T80 (s)
Pre-U69,593 T80
Post-U69,593 T80
Pre
Post

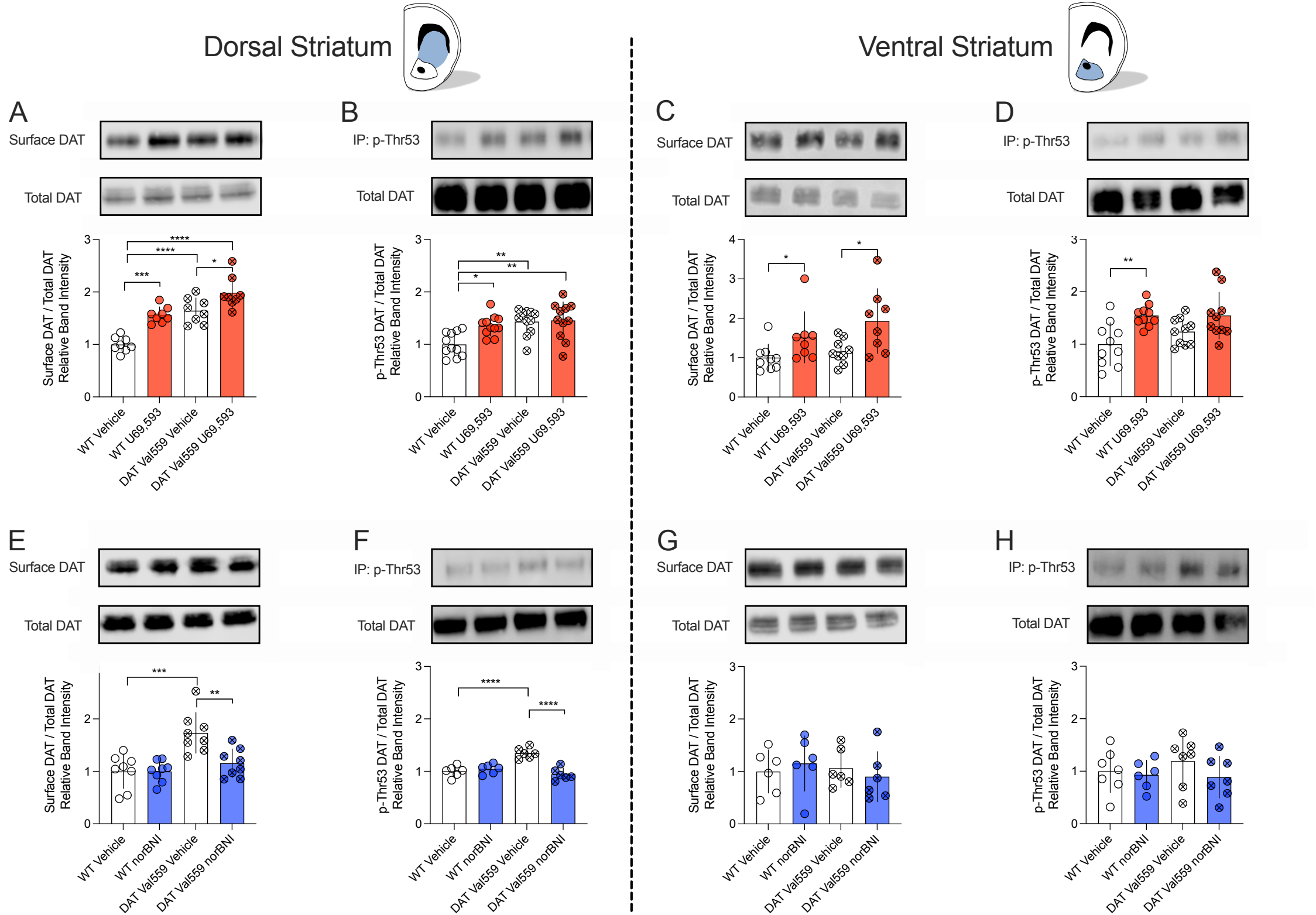
Dorsal Striatum
Ventral Striatum
A
Surface DAT
Total DAT
Surface DAT / Total DAT Relative Band Intensity
WT Vehicle
WT U69,593
DAT Val559 Vehicle
DAT Val559 U69,593
B
IP: p-Thr53
Total DAT
p-Thr53 DAT / Total DAT Relative Band Intensity
C
D
E
WT norBNI
DAT Val559 norBNI
F
G
H

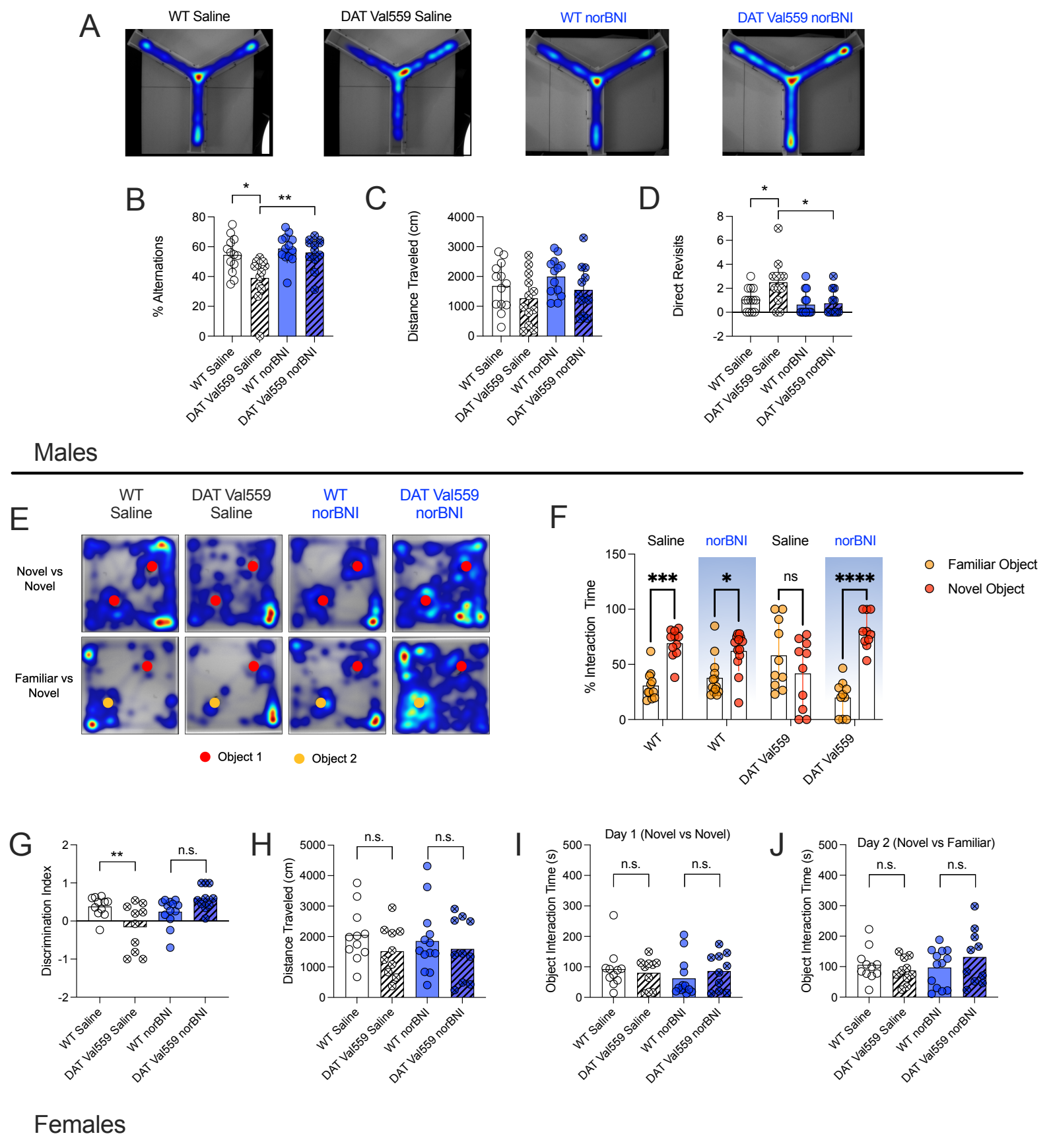
A
WT Saline
DAT Val559 Saline
WT norBNI
DAT Val559 norBNI
B
% Alternations
C
Distance Traveled (cm)
D
Direct Revisits
WT Saline
DAT Val559 Saline
WT norBNI
DAT Val559 norBNI
Males
E
Novel vs Novel
Familiar vs Novel
Object 1
Object 2
F
Saline
norBNI
% Interaction Time
Familiar Object
Novel Object
WT
DAT Val559
G
Discrimination Index
n.s.
H
Distance Traveled (cm)
I
Day 1 (Novel vs Novel)
Object Interaction Time (s)
J
Day 2 (Novel vs Familiar)
Females

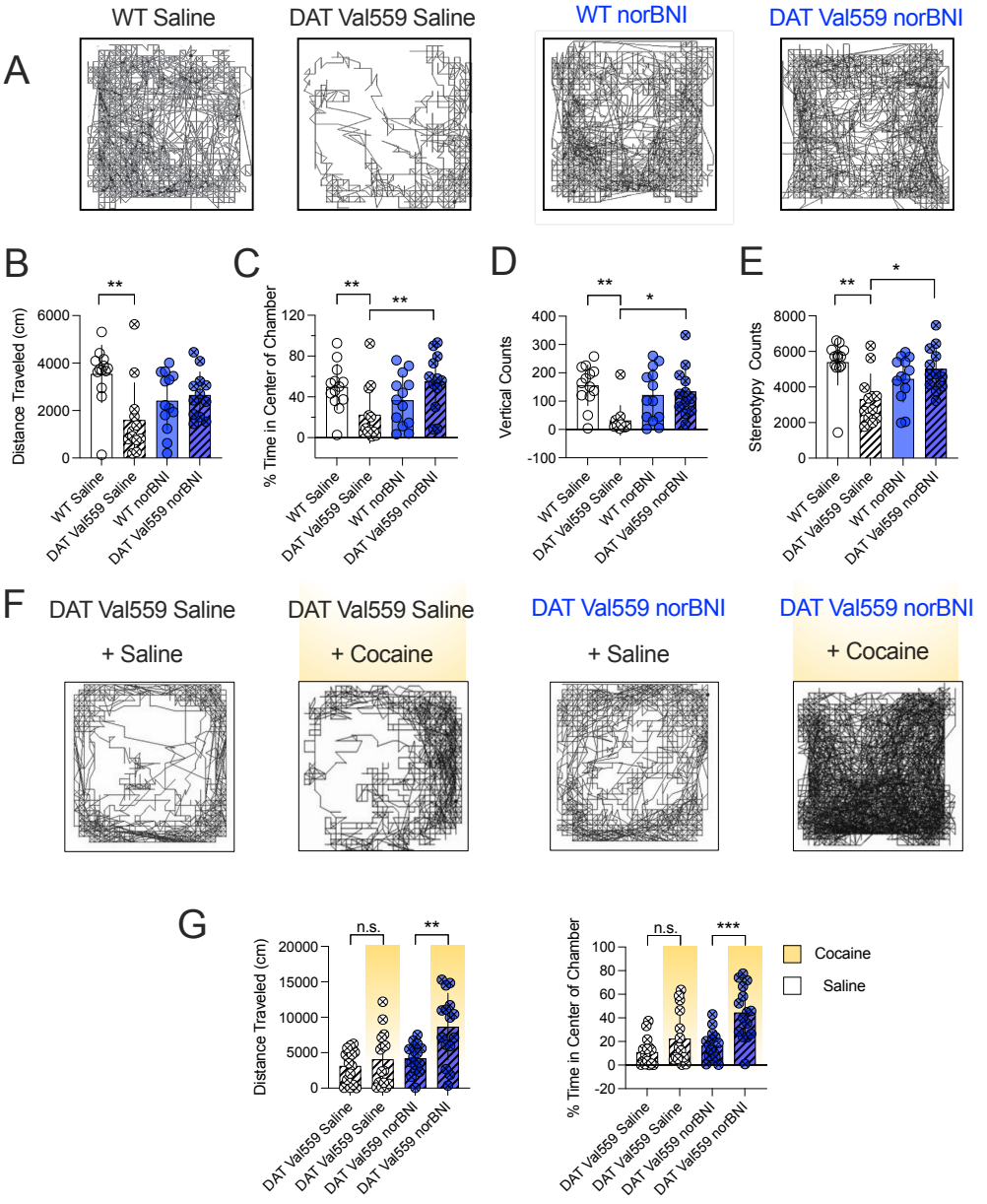
A
WT Saline
DAT Val559 Saline
WT norBNI
DAT Val559 norBNI
B
Distance Traveled (cm)
6000
4000
2000
0
**
WT Saline
DAT Val559 Saline
WT norBNI
DAT Val559 norBNI
C
% Time in Center of Chamber
120
80
40
0
**
**
D
Vertical Counts
400
300
200
100
0
-100
**
*
E
Stereotypy Counts
8000
6000
4000
2000
0
**
*
F
DAT Val559 Saline
+ Saline
DAT Val559 Saline
+ Cocaine
DAT Val559 norBNI
+ Saline
DAT Val559 norBNI
+ Cocaine
G
Distance Traveled (cm)
20000
15000
10000
5000
0
n.s.
**
DAT Val559 Saline
DAT Val559 Saline
DAT Val559 norBNI
DAT Val559 norBNI
% Time in Center of Chamber
100
80
60
40
20
0
-20
n.s.
***
Cocaine
Saline